Physico-chemical characterization of choline chloride based deep eutectic solvents used in CO_2 absorption and electrochemical conversion process

By Nishant Sharma

Technische Universiteit Delft

Physico-chemical characterization of choline chloride based deep eutectic solvents used in CO_2 absorption and electrochemical conversion process

By Nishant Manish Sharma

In partial fulfilment of the requirement for the degree of

Masters of Science
In Mechanical Engineering

At the Delft University of Technology
To be defended on Wednesday October 27, 2021 at 14:30.

Student number	4770218	
Daily Supervisor:	MSc. Hengameh Farahmandazad	TU Delft
Thesis committee:	Prof. dr. ir. W. de Jong (chair)	TU Delft
	Prof. dr. ir. E. Goetheer (co-chair)	TU Delft
	Prof. dr. R. Delfos	TU Delft

Abstract

Abstract Increasing CO_2 concentration in the atmosphere has caused significant concern, paving the way to research and develop technologies like capture carbon and storage (CCS) and carbon capture and utilization (CCU). This thesis focuses on extracting CO_2 from Chimney stacks and regenerating the solvent using electrochemistry. The main aim of this thesis is to identify a solvent that is capable of being used as a good CO_2 capture medium and at the same time as an electrolyte for CO_2 reduction.

Deep eutectic solvents (DES) have been gaining much attention due to their desirable properties such as biodegradability, low vapour pressure, and high tunability for the required purpose. Research has shown promising results in the application of DES in the field of CO_2 capture at a lower price with more eco-friendly solvent. Choline chloride is the most widely used quaternary amine salt which has all the desirable properties; when combined with a CO_2 philic hydrogen bond donor group such as amines, a novel solvent could be formed. The low/negligible vapour pressure of DES makes it suitable for CO_2 absorption in industrial applications. Based on the literature, three different solvents were selected, Choline chloride and Ethylene glycol (ChCl:EG), Choline chloride and Monoethanolamine (ChCl:MEA) and Choline chloride with Aminomethyl propanol (ChCl:AMP).

Various experiments were conducted on different molar ratios of selected solvents to determine the physico-chemical properties. Viscosity was measured as it affects the CO_2 absorption capacity due to limiting the mass transfer and has a significant impact on ion mobility resulting in high ohmic drops and reduced efficiency of the electrochemical extraction process. Conductivity was also measured as having higher conductivity will reduce the ohmic drop and improve the CO_2 removal process; conductivity is inversely related to viscosity. Effect of varying temperature, water and CO_2 loading was observed on these physical properties.

Based on the experiments conducted, it was found that ChCl:EG solutions have the highest conductivity among the pure solvents, with some of the lowest viscosities. In the case of ChCl:MEA, the viscosity reduced with the increase in temperature and increased drastically on the absorption of CO_2. This is because of the formation of carbamates as confirmed by FTIR. ChCl:AMP is a unique solvent as absorption of CO_2 results in the formation of a bicarbonate precipitate, as shown in FTIR.

Addition of EG to ChCl:MEA solution improves the performance of the DES significantly. At similar CO_2 loading, the viscosity of ChCl:EG:MEA (1:4:3) is almost 63.88% less and the electrical conductivity 134.45 % more than ChCl:MEA(1:6).

Acknowledgement

The past 10 to 11 months have been very special in various ways, I have been at the lowest and have bounced back to become stronger than ever before. This journey has given me a new sense of confidence and a strong purpose to move forward in life, achieve goals that I never thought would be possible, seeing new horizons. I take pride to admit that achieving a stronger mindset and this evolution that I experienced was not all my doing. I feel blessed and lucky to have known many people who were a part of my journey, helping and inspiring me along the way.

Hengameh Farahmandazad, you have been my mentor and an immense source of inspiration throughout my thesis. Thank you for putting your faith in me, answering all my questions and helping me understand basic concepts. Your enthusiasm for research is unmatched, all the discussions I had with you always filled me with confidence and a determination to achieve the results. All the discussions with you provided me with new knowledge and perspective. Thank you

I would like to thank Professor Wiebren de Jong for being my thesis supervisor. Your guidance and inputs from time to time have been monumental towards the work I have been able to do in this thesis. Thank you

I would also like to thank Professor Earl Goetheer for being my thesis chair. You have been a constant source of motivation for me, I would always look forward to my meetings with you. Your positivity pushed me to achieve more, thank you for taking time out of your busy schedule. Your belief in me gave me strength and urged me to do more. Thank you

Mom, dad and Nishtha, I dedicate my thesis to you. You have been the rock behind my back constantly supporting and showering me with love and support. You believed in me when I didn't believe in myself, I promised you that one day I will make my name I will keep that promise no matter what. I will make you proud.

Maitry Phukan, You are the most valuable person to me. You have supported me through my toughest times, you were the one who kept pushing me to achieve my goals when all felt lost. You have a very special place in my heart and I am grateful to have you as my partner. Thank you for holding me tight on my most vulnerable days. I love you so much

Ved Dhubhashi, you are a very close friend of mine and have become extremely important to me over the last year. You have seen my lowest points and been there to always support me in any way shape or form. You have helped me in more ways

than I can admit. Thank you for always being the rock in the stormy sea. It gives me a lot of strength knowing that I can rely on you and get your counsel when I am lost. Thank you
I would like a special thank to Mrigank Sinha for his guidance and support throughout my thesis. My deepest gratitude to Abhirath, Arya, Varun Kothari, Saloni, Anant, Marko, Stefan, Femke and Shashish for the love and care you have given to me. I could not have done it without you all.

Nomenclature

Table 1: List of molecules mentioned in this report

Molecules	Description
CO_2	Carbon dioxide
H_2O	Water
NaOH	Sodium Hydroxide
$BaCl_2$	Barium Chloride
$BaCO_3$	Barium Carbonate
KCl	Potassium Chloride
$RNHCOO^-$	Carbamate
$RNH_2^+COO^-$	Zwitterion
HCO_3^-	Bicarbonate
CH_4	Methane
N_2O	Nitrous oxide
$HOCH_2CH_2N^+(CH_3)_3Cl^-$	choline chloride

Table 2: List of abbreviations used in this report

Abbreviation	Description
PSA	Pressure Swing Adsorption
DAC	Direct Air Capture
TSA	Temperature Swing Adsorption
DES	Deep Eutectic Solution
CCU	Carbon capture and utilization
MEA	Monoethnaolamine
DEA	diethanolamine
MDEA	Methyldiethanolamine
AMP	Aminomethyl Propanol
ChCl	Choline Chloride
QAS	Quaternary Ammonium Salt
IL	Ionic Liquids
HBD	Hydrogen Bond Donor
HBA	Hydrogen Bond Acceptor
FTIR	Fourier-transforminfrared spectroscopy
VLE	Vapour Liquid Equilibrium

Contents

List of Tables

List of Figures

1

Introduction

The current world energy demands are primarily catered by the use of fossil fuels. Increased dependency on fossil fuels has to lead to an increase in the amount greenhouse gases such as CO_2 and CH_4 in the air [14] which has directly contributed to climate change. A number of efforts have been put forwards to fight climate change. One of the techniques that are currently showing promising results is carbon capture technique [15].

This chapter aims to describe the background and consequences of climate change. The presence of CO_2 gas in the atmosphere is one of the primary drivers of climate change. Thus, it is important to introduce the concentration and the sources of the emissions. Finally, it is important to establish the research gap and questions this thesis study aim to address.

1.1. Climate change

Many natural processes such as changes in solar energy, displacements of ocean currents and volcanic eruptions have been known to influence the climate. However, they cannot explain the most recently observed global warming trend. Since the start of the industrial era, human activities have contributed substantially to climate change by adding greenhouse gases to the atmosphere. In United States of America, average temperature has increased by 0.72^oC to 1.06^oC since 1895, and most of this increase has occurred since 1970 [2]. These gases come from a wide array of human activities such as fossil fuel burning to generate heat and energy, fertilization of crops, storage of residues in dumping sites, cattle, industry and industrial manufacturing.

1

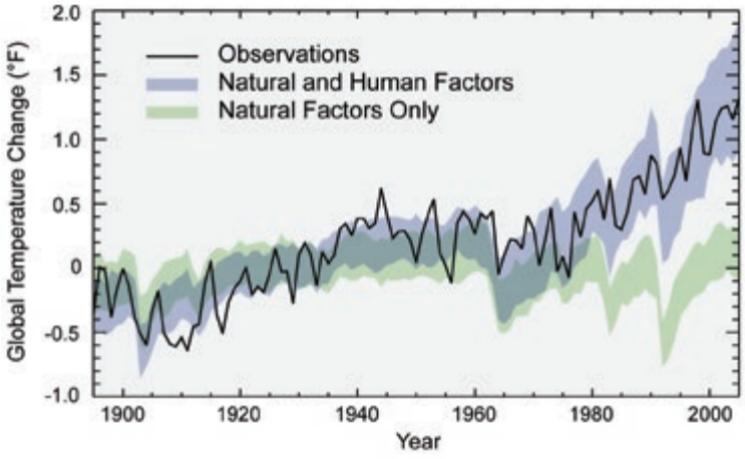

Figure 1.1: Effect of human activity on climate change expressed as global temperature change. Adapted from [2]

Figure 1.1 shows the change an increase in the global temperature over the course of the past century. The greenhouse gasses directly emitted by human activities are Carbon Dioxide (CO_2), Methane (CH_4) and Nitrous oxide (N_2O) which have accelerated the trend of the climate change.

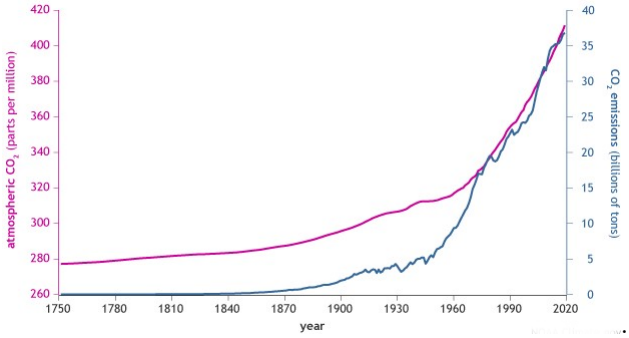

Figure 1.2: CO_2 concentration in the atmosphere and emission rate. Adapted from [3]

From Figure 1.2, we can observe that the amount of CO_2 in the atmosphere (pink line) has increased along with emissions (blue line) since the start of the Industrial Revolution in 1750. Emissions rose slowly to about 5 billion tons per year in the mid-20th century before skyrocketing to more than 35 billion tons per year by the end of the century [3]. There is a clear correlation between the increase in the atmospheric CO_2 concentration and the rise in the average global temperature.

1.1.1. Increase of CO_2 in air

CO_2 is the greenhouse gas that is the prime contributor to climate change. Although it is absorbed and emitted naturally as a part of the carbon cycle, human activities (especially burning fossil fuels) release excessive amounts, considerably increasing CO_2 concentration in the atmosphere.
Natural processes have varied atmospheric CO_2 concentrations from 170 to 300 ppmv. At present, the average concentration of CO_2 has increased to 412 ppm which is more than the expected 300 ppm [16]. The average global temperature at the surface of the Earth has increased by about 0.8 ^oC since 1880 [2]. Two-thirds of this growth has taken place since 1975. Based on the current trend it is predicted that the concentration of CO_2 can go as high as 600-700 ppm by the end of this century, which will intern cause a rise of about 4.5 - 5^oC on average[17].

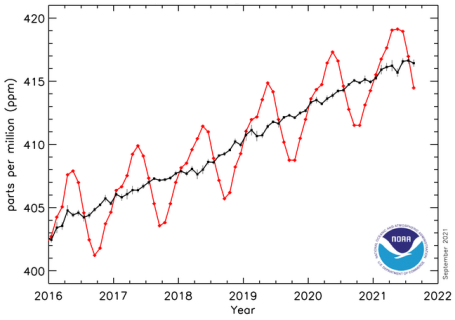

Figure 1.3: CO_2 concentration in ppm in atmosphere. Adapted from [3]

1.1.2. CO_2 Sources

Carbon dioxide is produced naturally by all living beings on this planet and some occasional natural occurrences which produce a large amount of CO_2 such as volcanic eruptions and wildfires. These are quite normal occurrences and do not cause any harm to the environment. Humans on the other hand have accelerated the production of CO_2 by many folds. According to statistics, power plants alone are responsible for about 40% of total greenhouse emissions. The transportation industry accounts for about 20% share in CO_2 emissions compared to 17% by agriculture sector [4]. Different sources of emit CO_2 in varying concentrations. The average concentration for CO_2 in the air is about 412 ppm. CO_2 has a very low partial pressure in air making direct air capture for CO_2 difficult. A more concentrated source for CO_2 would flue gas emitted from chimneys of coal or gas-fired power plants. Nepal et al observed and measure the CO_2 emission from brick kilns which are one of the largest producers of CO_2 in Nepal, on an average about 45-50 % vol of CO_2/vol of flue gas [18]. Adeyemi et al conducted an experimental study for CO_2 absorption at a partial pressure of 15 kPa which is also reported in other studies to be the partial pressure in many post combustion processes [19, 20].

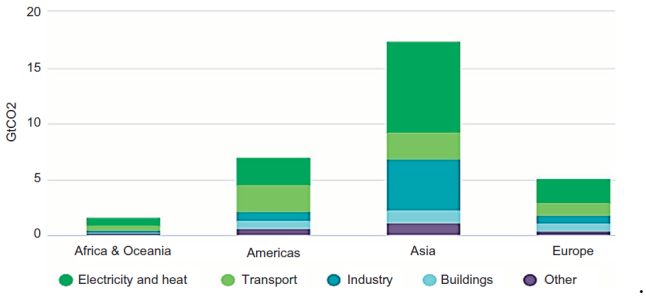

Figure 1.4: CO_2 emissions per sector in different continents in year 2019. Adopted from [4]

Figure 1.4 represents the main sources of CO_2 emissions from various sectors in different continents. The global emissions trend from 1990-2016 have shifted from the western to more Asian countries meaning that the developing countries like India and south east Asian countries along with China are now the leaders in carbon emissions across the globe especially after the year 2000.

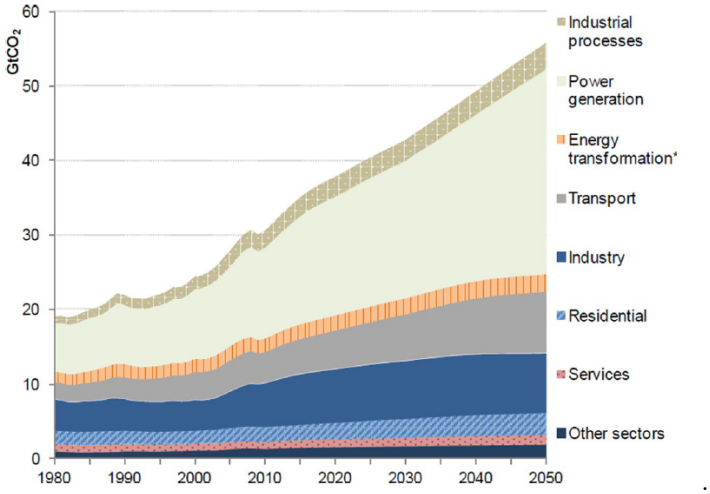

Figure 1.5: CO_2 emission trends. Adopted from [4]

1.2. CO_2 Capture technologies

This subsection deals with the existing carbon capture technologies, what are the advantages and limitations of these technologies.

1.2.1. CO_2 Capture strategies

CO_2 capture and storage is a promising technology and one that provides an immediate and long term solution to the problem at hand. Once the CO_2 is captured, it

can be separated from the solvent and could be stored in specific formations of the earth, or it can be used in other industries to make organic products. Broadly, this technology could be categorized into three different techniques: Pre-combustion, post-combustion, and Oxy-fuel combustion capture technology [5].

Pre-Combustion CO_2 capture

The Pre-Combustion CO_2 capture process involves the fuel to react with oxygen and steam(H_2O). This reaction results in the cracking of carbon to be converted into CO_2 and H_2; at the same time, a water-gas shift reaction will result in the conversion of carbon monoxide to carbon dioxide. The composition of the produced gas will be about 60-80% of Hydrogen and 20-40% of CO_2 [21]. Figure 1.6 represents a simplified diagram of how the pre-combustion process takes place.

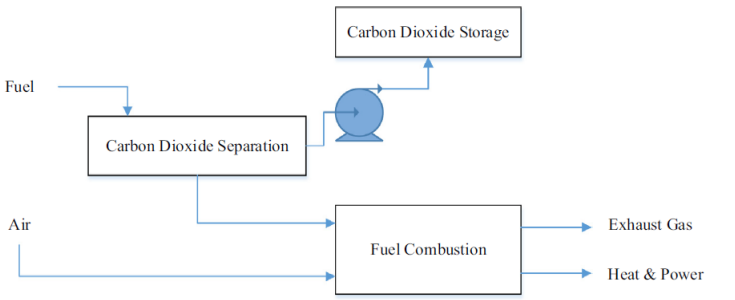

Figure 1.6: Schematic diagram of pre-combustion process. Adopted from [5]

Oxy-fuel combustion capture

In the Oxy-fuel combustion capture method, the fuel is burnt with pure oxygen, which leads to a higher concentration of CO_2 at the exit. The concentration of CO_2 is around 80% which results in higher partial pressure and hence higher absorption/adsorption[17]. Absorption/adsorption processes depend on the partial pressure of gas in a mixture, a higher concentration of CO_2 will result in higher partial pressure and hence, higher Absorption/adsorption.
This process is technologically feasible, but it consumes a large amount of oxygen from an intensive air separation unit, resulting in higher costs and a higher energy penalty. Energy penalty could be as high as 7% when compared to the energy consumption for a plant without carbon capture, and utilization [17].

Post-combustion capture

The process involves removing CO_2 from the flue gases coming out of the combustion process. The concentration of CO_2 is relatively low in this method, around 7-14% for coal-fired and as low as 4% for gas-fired plants [17]. Lower concentration results in higher energy penalty and associated cost for the capture unit. United States of America's national energy technology laboratory estimates that installing post-combustion capture technology in power plants will increase the cost of electricity production up to 70% [22].

1

1.2.2. CO_2 capture techniques

This section discusses the various methods used for capturing carbon dioxide.Various strategies have been discussed in the previous section. Figure 1.7 shows various methods to capture CO_2 that will be discussed in this section.

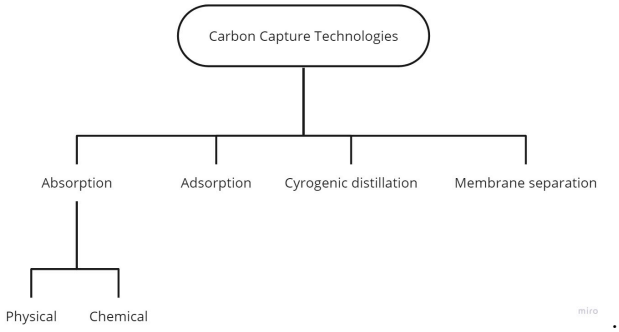

Figure 1.7: Different methods for CO_2 capture.

Membrane seperation

Various membranes are being used to allow only only a specific gas to pass through for instance membrane are capable of allowing CO_2 to pass through but block other gases like O_2 or N_2 or visa-versa. This method could also be used in the pre-combustion process as it is cable of removing oxygen and nitrogen from natural gas [17]. The development of high-efficiency membranes can produce CO_2 with 82-88% efficiency, whereas the development of ceramic and metallic membranes and polymeric membranes for membrane diffusion could produce a membrane with higher efficiencies than liquid absorption processes [17]. It is also important to point out that the performance of the membrane is heavily affected by the quality of flue gas, and operating conditions such as low CO_2 concentration and low pressure can significantly affect the efficiency.

Polymeric membranes: These membranes consist of a thin dense selective skin layered over a less dense porous support layer. The porous layer provides structural support enabling high-pressure applications. The higher performance of CO_2 separation could be achieved by increasing the solubility of CO_2 in membrane and increased diffusion of CO_2 through the membranes. Polysulfone is a chemically and thermally stable polymer for gas separation with high selectivity. Some other polymers include polyaniline, polypyrrolones, and polyarylates [23]

Inorganic membranes: due to stability at high temperatures, inorganic membranes have some advantages; they can be classified as porous and non-porous. Non-porous, such as palladium which is most commonly used to separate hydrogen, are generally expensive. Recent studies have shown that when adding a functional layer ratio, is added onto porous layer such as of silica or zirconia, higher CO_2 absorption is achieved [23].

Cryogenic distillation

This technique involves series of compression and cooling operations at sub-ambient temperatures and high pressure for separation of gaseous compounds either in pre-combustion or post-combustion stream [5]. This technology is widely used in producing highly pure liquid carbon dioxide. This is also used more prominently in pre-combustion process because of higher CO_2 concentration. Figure 1.8 shows the schematic diagram of the distillation process.

Cryogenic separation technology overcomes some shortcomings of conventional amine-based processes by avoiding excess water consumption, avoiding expensive chemical agents, corrosion, and foaming issues. This technology also allows the operator to be at ambient pressure condition and readily produces liquid CO_2 which is easier to manage and transport[5].

For CO_2 separation, flue gas is first cooled to desublimation temperature (173.15 to 138.15 K). The solidified CO_2 is then separated from other gases and is compressed to high pressure of 101.32 - 202.65 bar. This process typically recovers about 90-95 % pure CO_2 from the flue gas. The distillation is a highly energy-intensive process as it involves shallow temperature and high pressure resulting in energy consumption of about 600-660 kWh per ton of CO_2 produced [17].

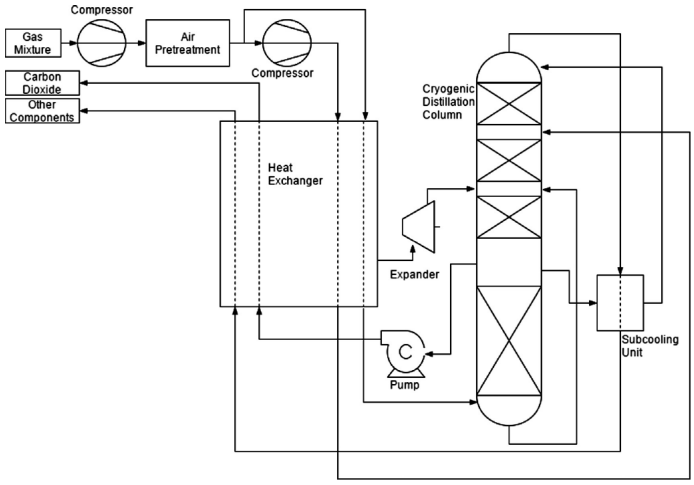

Figure 1.8: Schematic diagram of cryogenic distillation unit. Adopted from [5]

Adsorption

It is the process of adhesion of atoms, ions, or molecules called adsorbate to a surface called adsorbent. It is a physical process, in the case of carbon capture, as solid adsorbent is used to bind CO_2 to the surface. Typical adsorbents include molecular sieves, activated carbon, zeolites, calciumoxides, hydrotalcite, and lithium zirconate. The adsorbed CO_2 can be removed by swinging the pressure (PSA) or temperature (TSA) of the system. PSA is a commercially available technology that can have efficiency as high as 85% . In TSA, the CO_2 is released by increasing the temperature

using hot air. The generation time usually is more prominent than PSA, but the purity of CO_2 is higher roughly 95%, and recovery efficiency is higher than 80% [17]. In theory, the adsorption technique has been superior to others in higher loading capacity at ambient conditions. The process is less energy-intensive and economic regeneration process, mechanical and chemical stability, simple operation and maintenance, and good tolerance with moisture and impurities in the flue gas. The operating cost of a specific TSA process is estimated to be of the order 80-150 USD per ton of CO_2 captured [5, 17]

Absorption

Absorbing CO_2 using a liquid solvent from flue gas or DAC is a highly researched topic. Therefore it is the most matured method of CO_2 separation. Typical solvents include Monoethnaol amine (MEA), diethanolamine (DEA) and potassium carbonate. Once the solvent is loaded, the CO_2 can be removed from the system using a stripper or a regenerative process either by heating and/or depressurization [17]. A critical challenge of this technology is the degradation of solvent, resulting in solvent loss, equipment corrosion and generation of volatile degradation compounds. There are two primary forms of absorption techniques

Physical absorption: in this process, no chemical reaction takes place; the CO_2 is purely dissolved in the solution. High pressure and low temperature favour the reaction. Physical solvents such as Selexol, Rectisol and Fluor are favoured when the partial pressure of CO_2 in the flue gas is high [24]. Established physical solvent Selexol, i.e. a mixture of dimethyl ethers of polyethylene glycol (DEPG), is used for industrial applications. Figure 1.9 a shows a flow diagram for a physical absorption process using a DEPG solvent. CO_2 is first compressed using a two-stage compressor; the compressed gas is then passed through the DEPG solvent. The clean gas is collected on top, and the CO_2 rich solvent leaves from the bottom. The CO_2 rich solvent is passed through 3 flash tanks with decreasing pressures to regenerate the solvent, which is sent back to the absorber [6].

Chemical absorption: A liquid solution is used to separate CO_2 from the flue gas by selectively reacting with the gas. The CO_2 rich sorbent is regenerated by heating or by depressurizing the solution. This process is the most mature process for CO_2 absorption, and typical solvents include MEA, DEA, and potassium carbonate [17]. Among various alkanolamines, MEA has the highest efficiency for CO_2 absorption with the efficiency of over 90% [25], An absorption pilot plant with 1 Ton CO_2/h has been constructed and successfully tested with the post-combustion capture technology for a coal-fired power plant using a solvent containing 30% MEA [26]. Figure 1.9b depicts the chemical absorption process using MEA solvent. In the process, the flue gas is first cooled and passed over a 30 wt% MEA water solution. The CO_2 from the flue gas is dissolved into the solvent via chemical reactions, which are discussed later in the report. Clean gas is then removed from the top, and CO_2 rich solvent is collected at the bottom, which is then sent to a stripper for desorption to regenerate the solvent via heating, and distillation [6].

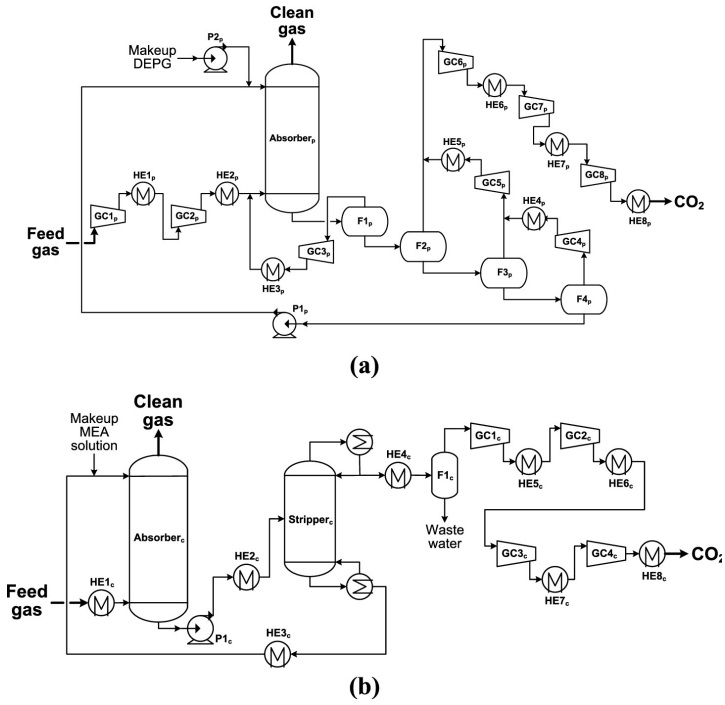

Figure 1.9: Flow sheet for physical absorption (a) and Chemical adsorption using MEA solvent (b). Adopted from [6]

1.2.3. Electrochemical conversion of CO_2

CO_2 is one of the most stable carbon-based structures to exist in environmental conditions. Hence, the biggest challenge posed to the technologies mentioned above is CO_2 removal. The CO_2 once adsorbed/absorbed in the solvent is removed using a regenerative process which is either driven by temperature or pressure; the main drawback of these processes is a high cost associated with them (60-107 USD / ton of CO_2) [27]. Electrochemical reduction of CO_2 is an exciting alternative to remove CO_2 from the solvent. This method selectively oxidises a gas at one electrode into an ion transported through a liquid electrolyte to the other electrode, where a reduction reaction occurs. The advantage of this method is that separation occurs at a lower temperature and pressure compared to existing technologies and, in principle, requires less energy [28]. Electrochemical reduction of CO_2 is an attractive strategy; not only the conversion takes place near room temperature at ambient pressure conditions but depending on the catalyst, electrolyte, and reaction condition, various products could be formed at different conversion rate [29].

CO_2 separation using electrochemical process has shown relevance in a wide range of applications and has the potential to become more and more relevant in the coming years. Early studies in this field have shown incredible potential; there is however significant research and development potential work required in order to reduce cost and improve performance [30].

1

1.3. Ionic liquids

Ionic liquids (IL) are salts with a melting point usually lower than water (100 ^oC). They are composed of organic cations and organic/inorganic polyatomic anions. IL dates back to 1914 when the preparation of ethyl ammonium nitrate using a concentrated nitric acid and ethylamine resulted in a pure salt after removing water. This salt was liquid at room temperature[31]. The notable advantage of using IL is that they can be tuned to desired properties, and the formation of the desired cation and anion exchange is a crucial step in IL's formation [7].

IL's can be used as a potential alternative for CO_2 capture owing to their unique characteristics. There are also additional benefits of lower melting point, frequently negligible vapour pressure, as well as high chemical and thermal stability along with the solvents being non-flammable [14]. During the past decade, IL-CO_2 systems have been studied in great detail. Conventional IL has been synthesised in a way that they do not possess any functional groups, and thus, CO_2 absorption occurs through a physical absorption mechanism. The CO_2 absorption capacity of ILs can be improved by functionalisation of ILs, using binary mixtures of ILs, or mixing ILs with selected organic solvents [14].

The synthesis of IL is complicated as it requires a large amount of expensive raw materials, and the process is seldom environment friendly. This limits the scope and industrial application for IL. In order to cope with the high price and toxicity related to IL, a new generation of solvents is introduced within the last decade called Deep Eutectic Solvents [1]. A new generation of ILs has emerged a little over a decade ago concerning the cost and impurities associated with water. These ILs are called Deep Eutectic Solvents (DES).

1.4. Deep eutectic solvents

DES is synthesised by mixing two components with an appropriate molar ratio to form a eutectic solution with a freezing point lower than each component. This reduction in freezing point is because of the strength of interactions between the two individual components [14]. DES have similar properties to IL and are synthesised by mixing a lewis acid, and a base [7]. In general, these solvents exhibit properties, such as economic availability, biodegradability, recyclability, non-flammable, biocompatibility, non-toxicity, high thermal stability, and non-volatility. DESs are considered as economical alternatives to standard ILs because their preparation is more straightforward with higher purity and low-cost on a large-scale [32, 33].

The formation of DES depends on the magnitude of the interaction between individual components. Figure 1.10 depicts the interaction between components A and B. Unlike theoretical ideal mixtures, these interactions result in a considerable value of ΔT_f. Eutectic point is reached when the correct molar fraction(ratio) of A & B is achieved at a specific temperature. At this point, the melting point, depression is observed as shown in the figure 1.10 [7].

In general, DES can be categorised into four different categories as depicted in Table 1.1. In type III DES, the CAT^+ depicted in the table is usually quaternary ammonium, phosphonium or sometimes sulfonium salt. The X^- is the anionic moiety

involved in hydrogen bonding with the protons from the RZ donor group[1]. Choline Chloride is the most widely used quaternary ammonium salt due to its low cost, availability, biodegradability and low toxicity. The chloride anion is readily available to interact with a diversity of proton donors through hydrogen bonding[7].

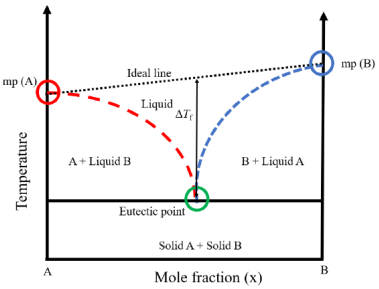

Figure 1.10: T-X diagram for DES. Adopted from [7]

Table 1.1: General formula for DES classification. Adopted from [1]

Type	General Formula	Terms
Type I	$Cat^+X^-zMCL_x$	M= Zn,Sn, Sl, Ga, In
Type II	$Cat^+X^-zMCL_x.yH_2O$	M= Cr, Co, Cu, Ni, Fe
Type III	Cat^+X^-zRZ	Z= $CONH_2$, COOH, OH
Type IV	$MCl_x + RZ = MCl^+_{x-1}.RZ + MCl^-_{x+1}$	M= Al, Zn and Z= $CONH_2$, OH

As discussed, DES is synthesized by mixing a hydrogen bond donor (HBD) and a hydrogen bond acceptor (HBA). Many potential combinations result in tenable physico-chemical properties such as conductivity, viscosity, polarity, and thermal properties. This tenability can be achieved simply by changing the molar ratios of the constituent materials; most of the DES synthesized are hydrophobic [1, 7, 14].

1.4.1. Choline chloride

2-Hydroxy-ethyl-tri-methyl-ammonium cation or $HOCH_2CH_2N^+(CH_3)_3$ commonly known as choline chloride has a structure as shown in figure 1.11. Choline chloride is biodegradable, non-toxic and cheap to manufacture. It is classified as a pro-vitamin in Europe. It is produced on the mega-tonne scale as an animal feed supplement. It is produced by a one-step gas-phase reaction between HCl, ethylene oxide, and tri-methyl-amine and, as such, produces little ancillary waste [7, 8]. Many of the properties of choline based DESs are similar to conventional ILs, except for the decomposition temperature, heat capacity, and ecotoxicity. The lower heat capacity of these solvents contributes to lower sensible heat with increased temperature, which leads to lower energy usage in the CO_2 separation process. The non-ecotoxicity,

biodegradability, and low cost of choline chloride-based DES indicate an excellent use for an alternative eco-friendly CO_2 capture medium [34]. Choline chloride is the primary focus for this thesis; choline chloride-based DES has shown great potential for CO_2 adsorption with good electrical conductivity, which is suitable for electrochemical conversion because of lower ohmic losses. Amine based DES has been considered as well for the study due to higher CO_2 absorption.

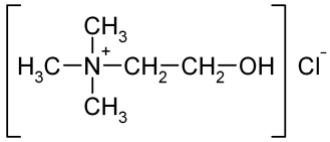

Figure 1.11: Chemical structure of choline chloride

1.5. Research Objective

The main objective of this research is to explore and find a solvent which is cable of using as a CO_2 capture medium and simultaneously as an electrolyte in the electrolyser to convert CO_2 electrochemically. In order to address the aim of the thesis, following research questions needs to be answered:

- Which type of DES will be the most suited for the two processes, CO_2 capture medium and electrolyte for CO_2 reduction?
- What are the physico-chemical properties of the selected solvent?
- What are the limiting factors for the performance of the selected solvent?

With the knowledge obtained from the research questions mentioned above, the final objective of the thesis is to improve the performance of the selected solvent for CO_2 and eletrochemical conversion.

1.6. Thesis scope

characterisation of the of a solvent is an exploratory task. Therefore, it is necessary to define the scope of research before hand

- It is important to note that the process involved in this thesis study is the extraction of CO_2 from chimney stacks. The choice is made for not going for DAC is because this technology is in its infancy, and enough is not known about the CO_2 absorption characteristics of the solution.
- This project is solely done from an absorption standpoint, and desorption or life cycle characteristics are not investigated. Electrochemical desorption criteria are considered, but this is not a comprehensive study on the electrochemical conversion process.

- Even though the absorption of CO_2 is dependent on a several parameters and physical properties of the solution, not all properties could be measured due to limited time and equipment availability.

2

Background

The following chapter commences with an introduction to deep eutectic solvents. After that, the introduction of the amine group and how DES can be used for CO_2 absorption. Subsequently, these solvents' physical and chemical properties and how various parameters affect these properties are discussed.

2.1. Deep eutectic solvents

The terms deep eutectic solvents and ionic liquids have been used interchangeably quite frequently, but it is necessary to point out that there are two different types of solvents. DESs are formed from a eutectic mixture of a Lewis or Bronsted acid and a base containing various anion and cationic species. On the other hand, ionic liquids are formed from one type of discrete anion and cation system. It is essential to bring to attention that the physical properties of DES are similar to ILs [8]. Deep eutectic solutions have been mainly classified into four categories as shown in table 1.1. In this study, we will primarily focus on type III eutectic solutions formed from choline chloride, which acts as a HBA [1, 35]. These solvents are interesting due to their ability to form a DES with a large variety of HBD. These are simple to prepare, relatively low cost and biodegradable. A wide range of HBD means this class of DES are remarkably adaptable [8, 35]. A wide range of DES solvents has been studied with solvents formed using amides, carboxylic acid and alcohols. Figure 2.1 gives some possible solvents with their HBD and HBA. These solvents are easy to prepare, relatively unreactive and cheaper than most ionic liquids. This wide range of HBD means that these solvents are highly tune-able [1].
DES contains large non-symmetric ions that have low lattice energy, which results in lower melting points[8]. The delocalization of the charge through the hydrogen bond between the salt and the hydrogen bond donor is responsible for the reduction in melting point[36]. When a range of quaternary ammonium salts are heated with $ZnCl_2$, the freezing point of the resulting liquids was found to decrease considerably. The salt ammonium salt which caused the lowest melting point was choline chloride

[36]. This initial study has now been extended, and a large variety of salts and hydrogen bond donors have now been developed [35].

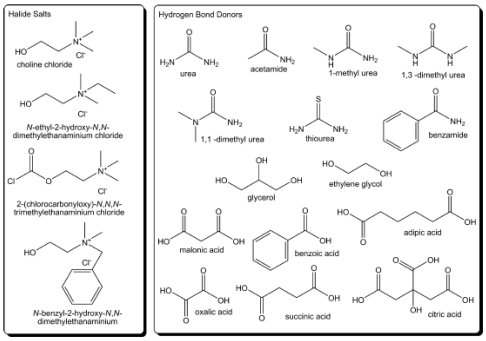

Figure 2.1: Possible HBD and HBD for DES. Adopted from [1]

Choline Cloride-Ethylene Glycol DES

In the light of recent years, DESs are seen as a potential environmental friendly medium for CO_2 capture. A number of solutions could be made using Choline Chloride as the QAS, choline chloride-Urea, and choline chloride-ethylene glycol are the two most popular solutions [8]. Zhang et al. studied sixteen choline chloride-based DES for their thermodynamic properties, choline chloride-ethylene glycol DES has shown promising results [34].

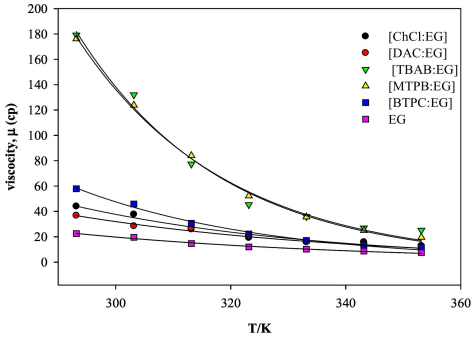

(a) Comparing viscosity data for ehylene glycol based DES. Adopted from [37]

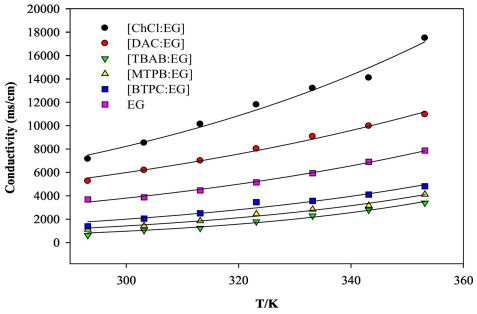

(b) Comparing electrical conductivity data for ehylene glycol based DES. Adopted from [37]

Figure 2.2: comparing viscosity and conductivity data for EG based DES

Viscosity is a significant concern associated with the industrial application of DES, especially for CO_2 separation. Figure 2.2a shows the viscosity data for an EG based DES; it can be observed that viscosity for ChCl:EG is relatively low compared to other solvents. Viscosities for choline chloride-based DES vary from 4 to $75 * 10^4$ mPa.s as studied by Zhang et al. [34]. Viscosities of choline chloride-based DES is similar to conventional IL; choline chloride ethylene glycol has a viscosity of about

39.9 mPa.s at 298K temperature [8, 34]. Comparing this to other choline chloride-based DES, this is moderately low; another solvent such as ChCl:Urea has a viscosity of 1372 mPa.s, which is relatively high. The thesis aims to find a solution that acts as a both CO_2 capture medium and an electrolyte, and electrical conductivity is highly dependent on viscosity as discussed in section 2.4.5 a solution with lower viscosity is desired. Figure 2.2b shows the conductivity of the ethylene glycol-based DES solution; it can be observed that the conductivity of this solution is relatively high. Abbott et al. used Hole theory to explain the relationship between the conductivity of the DES and viscosity, which will be discussed in section 2.4.4, the conductivity of ChCl:EG was found to be 7.61 mS/cm [8, 35, 38]. This, when compared to ChCl:Urea is quite significantly higher as could be seen in figure 2.3. KCl is a standard calibration solution and has a relatively high conductivity of about 11.88 mS/cm at room 293.15 K. This thesis aims to find a solution with conductivity as close to KCl solution as possible. Lower conductivity results in higher Ohmic losses which will drastically increase the cost of CO_2 extraction process. The lower limit for the electrical conductivity of the solution is set at about 3 mS/cm.

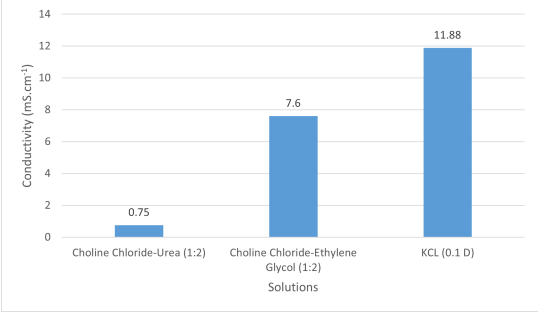

Figure 2.3: Comparison of conductivity for various solution. Adopted from [8]

2.2. Amines

Amines have been synonymous with carbon capture ever since the early stages of technology. Amines are preferred for carbon capture because of their high affinity towards CO_2 [39]. Industries use alkanolamines such as monoethanolamine (MEA), diethanolamine (DEA), N-methyldiethanol amine (MDEA) and 2-amino-2-methyl-1-propanol (AMP)[39]. Generally, amines are classified into three different categories: Primary, secondary, and tertiary amines. The classification is made based on the number of alkyl groups attached to the nitrogen atom. Figure 2.4 shows the various types of amine configurations where alkyl groups are represented by R, nitrogen atom by N and hydrogen bonds are represented by H.

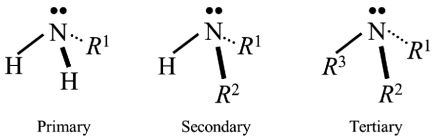

Figure 2.4: Different type of amines. Adopted from [9]

The choice of amines depends highly on the process involved and is heavily influenced by the operation parameters. Figure 2.5 shows popular amines structures, and their products after reaction with CO_2; primary and secondary amines such as MEA and DEA have a distinct advantage of forming stable carbamates. Conversely, carbamate formation increases the regeneration cost of the solvent [39]. The Zwitterion mechanism indicates that the primary and secondary amine first reacts with CO_2 to form zwitterions, and the intermediate is instantly neutralized by base (such as amine, OH^-, or H_2O) to form carbamates [40, 41]. Equation 2.2 shows the reaction for carbamate formation.

$$CO_2 + RNH_2 \rightleftharpoons RNH_2{}^+COO^- \tag{2.1}$$

$$RNH_2{}^+COO^- + RNH_2 \rightleftharpoons RNHCOO^- + RNH_3{}^+ \tag{2.2}$$

Figure 2.5: Products of amine reaction with CO_2. Adopted from [10]

Absorbent	Molecular structure of species	
	Free amine	Carbamate, bicarbonate/carbonate
MEA		
DEA		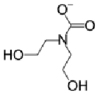
TEA	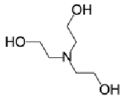	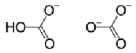
AMP		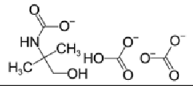

Tertiary amines such as TEA, as seen in figure 2.5 have low reactivity to CO_2 because of the additional step of formation of bicarbonate from carbamates in the presence of water as shown in equation 2.3. This is beneficial as it results in lower regeneration cost [9, 39]. Along with this, the theoretical loading capacity of tertiary amines is 1 mol of CO_2 per mole amine compared to 0.5 mol CO_2 per mol amine for primary or secondary amine [39].

$$RRNHCOO^- + H_2O \rightleftharpoons RRNH + HCO_3{}^- \tag{2.3}$$

Another class of amines is known as sterically hindered amine, a prime example of this is AMP. AMP is a hindered form of MEA, as can be seen in figure 2.5. Such a structure is obtained by substituting two hydrogen atoms attached to the α-Carbon atom to the amino group in MEA by two methyl groups; this substitution significantly affects the amine groups properties, and absorption capacity [39]. The reaction of sterically hindered amine is similar to primary amines as shown in equation 2.2. Due to the hindrance of the bulky amino groups adjacent to the nitrogen atom, the AMP-carbamates formed are unstable. Hydrolysis of these unstable carbamates results in the formation of bicarbonates as shown by equation 2.3. In theory, AMP can have maximum absorption of 1 mol CO_2 per mol of amine. AMP reaction has faster kinetics of the reaction compared to tertiary amines, and low solvent regeneration cost offers an industrial application advantage [39].

2.2.1. Monoethanol Amine DES

Many DES have been reported to have the potential for significant capacity of carbon storage such as Choline Chloride- Ethylene Glycol as mentioned in the previous section [42]. These Solvents can be used for high pressure CO_2 extraction. However, in the recent study, an aqueous mixture of choline chloride:Urea (1:2) and monoethanolamine was observed to absorb CO_2 for the pressure of 900 KPa. The findings also show the potential of improving the CO_2 absorption with alkanolamines [43].

Monoethanol (1-Aminoethanol) is known to form DES with various HBA. In the present study the QAS, Choline Chloride acts as the Hydrogen Bond Acceptor and Monoethanol amine acts as the Hydrogen Bond Donor. Figure 2.6 represents the molecular structure for DES [12].

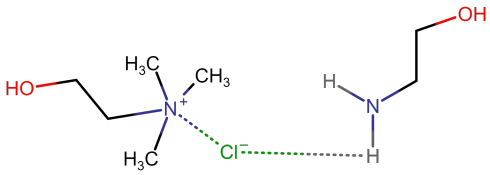

Figure 2.6: Choline Chloride Monoethanolamine DES structure

The number of hydrogen atoms on MEA is one more than DEA (secondary amine) or any other Tertiary amine, making MEA a better Hydrogen Bond Donor than other amines. This also results in a faster reaction with CO_2 making the kinetics of the reaction faster[12]. The main aim of the research, along with increasing the carbon absorption capacity for the DES. Figure 2.7a represents the various molar ratios and the respective viscosities at different temperatures. It can be seen that increasing the molar ratio reduces the viscosity. ChCl:MEA (1:5) shows the highest value for viscosity at 298.15K to be 0.0485 Pa.s which decreases to 0.0327 Pa.s when

molar ratio is 1:8 [11]. Figure 2.7b shows the reduction in density as we increase the molar ratio.

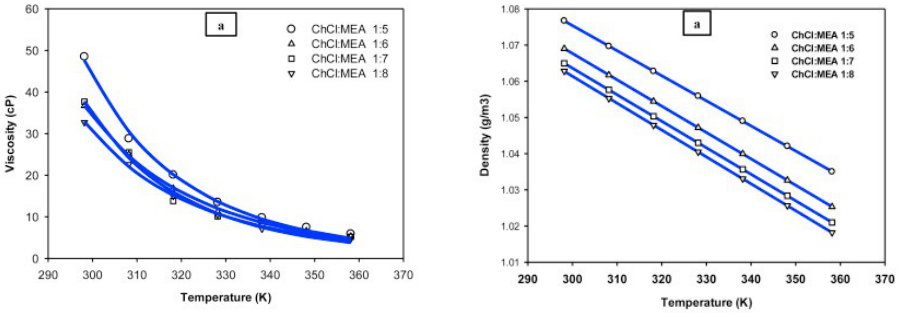

(a) Viscosity comparison

(b) Density comparison

Figure 2.7: Comparing viscosity and density of ChCl:MEA with different molar ratios. Adopted from [11]

The next thing that was considered while choosing the molar ratio is CO_2 absorption. Li et al. compared three different amine-based DES varying the HBA [12]. Based on the experiments performed, it can be observed from figure 2.8 the effect of molar ratio on CO_2 absorption. As the molar ratio of MEA is increased, the CO_2 absorption increases and then reaches a plateau after 1:4, indicating that 1:4, 1:5, and 1:6 molar ratios have identical loading capacities. Based on the literature on other amines, the viscosity of amines increases drastically after the formation of carbamates upon reaction with CO_2. Currently, there is no available literature on how the viscosity will change as CO_2 is absorbed. This thesis study aims to understand the relationship between the amount of CO_2 absorbed and how it affects the physical parameters such as viscosity and electrical conductivity. It is also important to point out that there is a gap in the literature with regards to the electrical conductivity of the ChCl:MEA DES, which will also be studied in this thesis study. Based on these results, molar ratios of 1:5 and 1:6 seems to be the most suited solutions for this thesis study since they have viscosities comparable to ChCl:EG solutions and have great CO_2 loading capacities.

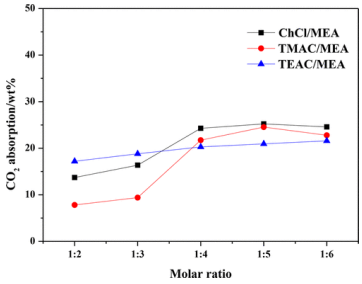

Figure 2.8: Comparing different molar ratios and CO_2 absorption. Adopted from [12]

2.2.2. Aminomethyl propanol DES

AMP also known as 2-amino-2-methyl-1-propanol is chosen for this thesis study. It offers high absorption selectivity to CO_2 absorption and degradation Resistance over conventional amines [44, 45]. As discussed in the section 2.2, AMP is a satirically hindered amine which is forms unstable carbamates, and in the presence of water, it forms bicarbonate. Lower heat of desorption and higher reaction kinetics makes it suitable for industrial application. AMP DES has not been studied yet; this thesis study will aim to form a DES with choline chloride as the QAS and try to characterise the properties exhibited by this DES.

2.3. Absorption

Absorption is a process by which gaseous substances mix into liquid solvents. Absorption can be classified into two distinct categories physical absorption and chemical absorption.

2.3.1. Physical absorption

Physical absorption is bounded by weak Van der Waals forces between the molecules. The absorption is governed by Henry's Law which states that at a constant temperature, the amount of gas dissolving in a given solution is directly proportional to the partial pressure of the gas in the vapour-liquid equilibrium [13]. In general, gas is absorbed at a higher pressure and desorbed at lower pressure maintaining a constant temperature for solvents that use physical absorption. Since the absorption and desorption are a factor of pressure, the loading and unloading of the sorbent could be done using a pressure swing setup which requires much less energy compared to chemical absorption, and desorption process [46]. Conventional DES such as Choline Chloride and Urea or Ethylene glycol use physical absorption to capture CO_2 whereas amines lean to chemical absorption for capturing CO_2.

2.3.2. Chemical absorption

Chemical absorption of chemisorption is the result of chemical bond formation due to the reaction between the reactants. This process is suitable for a low-pressure, low-temperature system. However, it still follows Henry's law, and higher pressure will result in higher kinetics of the reaction. Regeneration of the solvent is an energy-intensive process since, in most cases, the reaction produces chemically stable compounds. To recover the individual reactants, we need to shift the vapour-liquid equilibrium by increasing the temperature or reducing the pressure; this naturally results in higher energy demand in the desorption process. Amines generally react with the CO_2 to form carbamates or bicarbonates depending on the type of amines as discussed in section 2.2 [39].

2.3.3. Physics of absorption

The chemical reaction between CO_2 and amines is an exothermic process and hence favours lower ambient temperature. To understand the absorption process, it is essential to understand the Two film theory. The two-film theory describes the

mass transfer of a solute from one phase to another, which involves mass transfer from a gas phase to a liquid phase. This theory helps us to understand the mass-transfer limitations and each films resistance to the mass-transfer [13]. From the theory, maximum resistance to the mass transfer is limited to a very thin region at the interface called the film. A steady-state profile is assumed, meaning there is no accumulation of mass at the gas-liquid interface. Another major assumption in theory is that the liquid is non-volatile, and thus the reaction only takes place in the liquid film or inside the bulk.

In the case of amine-based absorption, the process initiates with the CO_2 getting diffused in the amine-air interface. This is followed by the dissolution of CO_2 in the amine; this does not indicate the formation of carbamates. After dissolving, the CO_2 molecule starts to react with the Liquid sorbent and relevant products are formed. A concentration gradient is established in the liquid phase, as CO_2 molecules are limited by diffusion in the solvent due to an increase in density and viscosity; because of the formation of carbamates which are significantly bigger molecules and produce hindrance to the flow. This change in viscosity is discussed in detail in section 2.4.4.

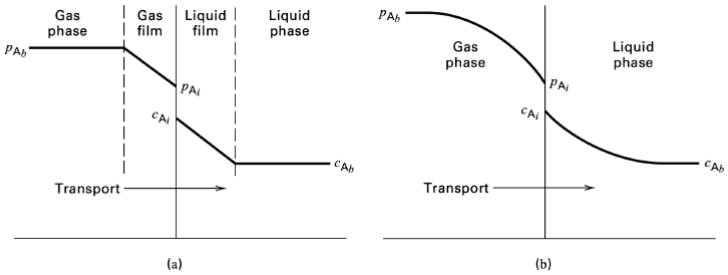

Figure 2.9: Schematic diagram of two film theory. Adopted from [13]

In figure 2.9, the diffusion in the first part of the gas film (air-amine interface) happens due to a concentration gradient. This diffusion is determined by the law of diffusion as proposed by Fick in 1855 called Fick's law of diffusion. This law derives inspiration from Fourier's law of heat conduction which shows proportionality between heat flux due to conduction and temperature gradient. Similar to heat diffusion, Fick's law shows proportionality between molar flux by molecular diffusion and concentration gradient. The law is described by the following equation 2.7 [13]. Equation 2.4 Shows the rate of in terms of mass transfer coefficients, the concentration gradients in the equation could be visualised from the figure 2.9. Equation 2.5 gives the mass transfer rate in the gas phase under dilute or equimolar counter diffusion conditions (EDM) and equation 2.6 gives the mass transfer rate in the liquid phase [13].

$$N_A = \frac{(D_{AB})_G}{\delta_G}(C_{A_b} - C_{A_i})_G = \frac{(D_{AB})_L}{\delta_L}(C_{A_i} - C_{A_b})_L \tag{2.4}$$

$$N_A = K_p(p_{A_b} - p_{A_i}) \tag{2.5}$$

$$N_A = K_c(C_{A_i} - C_{A_b}) \tag{2.6}$$

where,
N_A = Rate of mass transfer [mol/s]
δ_G = Thickness of gas film layer [m]
δ_L = Thickness of liquid film layer [m]
D_{AB} = Diffusion coefficient $[m^2/s]$
C_{A_i} = Molar concentration at the interface [mol/m]
C_{A_i} = Molar concentration in the bulk [mol/m]
p_{A_i} = Partial pressure at the interface [Pa]
p_{A_b} = Partial pressure in the bulk [Pa]
K_c = Liquid phase mass transfer coefficient [m/s]
K_p = Gas phase mass transfer coefficient [mol/s-Pa]

$$J = -D\frac{d_{c_A}}{d_z} \tag{2.7}$$

where,
J= Diffusion flux $[mol/m^2s]$
D= Diffusion coefficient $[m^2/s]$
$\frac{d_{c_A}}{d_z}$ = Molar concentration gradient $[mol/m^3.m]$

Once the CO_2 molecule moves into the bulk of liquid, the absorption is again limited by diffusion but this time due to the liquid surrounding the molecule. This diffusion can be quantified by the Stokes-Einstein equation 2.8, which relates the diffusion through a liquid of low Reynolds's number.

$$D = \frac{k_b T}{6\pi\mu r} \tag{2.8}$$

where
D = Diffusion constant $[m^2/s]$
T = Temperature of liquid [K]
k_b = Boltzmann constant $[m^2kg/s^2K]$
μ = Dynamic viscosity [kg/ms]
r= Radius of sphere molecule [m]

As we can see from the equation 2.8, diffusion is inversely proportional to the viscosity. Hence, with the increase in viscosity, the diffusivity decreases. In amines, formation of carbamates/bicarbonates leads to an increase in viscosity, resulting in the decrease in diffusivity limiting the overall CO_2 loading capacity.

2.4. Physical properties

Physical properties of a solution play a crucial role in identifying its application. It is important to establish some important physical parameters and how each of them affect the others. This section explores the dependence of various parameters and how each of them could be used to identify the most suitable solvent for the process.

2.4.1. Freezing point

One of the most important characteristics of the DES is the fact that the freezing point of the mixture is lower than that of the individual components. The depression of the freezing point is due to the establishment of strong intermolecular interactions between the HBD and HBA pairs and the optimal eutectic mixture composition. [8, 14, 35]. Figure 2.10 represent the eutectic composition of a binary mixture of A and B, ΔT_f represents the difference in temperature theoretical melting points of the two components and melting point of the eutectic solution. The larger the interaction between the HBD and HBA, the higher the value of ΔT_f [8]. The freezing point is also influenced by the Lattice energy of the salt and the HBD and the entropy change occurring in the formation of the solution. DESs, which are constituted of larger ions with smaller charges, needs less energy to break the bonds, causing a minor depression in the freezing point [14, 47]. Comparatively a halide salts with a low freezing point can form complexes with the HBD and form a lower freezing point solution. For examples, a mixture of ChCl:Urea (1:2) has a freezing point of 235K, significantly lower than the individual components, Choline Chloride has a melting point of 575K and Urea has a melting point of 406K [14]. Table 2.1 gives the value for the freezing point of selected DES from the available literature

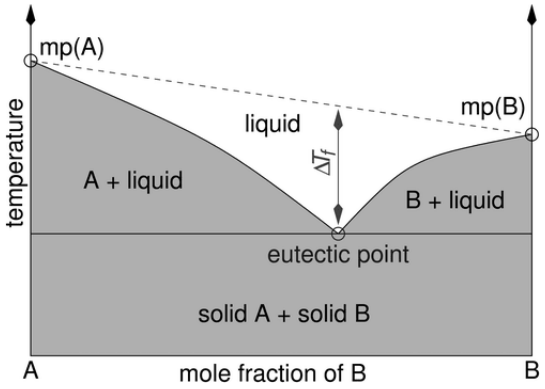

Figure 2.10: Schematic representation of two-phase component diagram. Adopted from [8]

2.4.2. Density

Density is one the most important physical properties for ionic liquids and in general DES in particular, the density of the solution is highly dependent on the type of

Table 2.1: Literature value for Freezing point of DES

Solvent	Melting point (k)
ChCl:EG (1:2)	<253.15
ChCl:MEA (1:5)	276.45
ChCl:MEA (1:6)	276.45

salt used [14]. Mjalli et al. conducted simulation and experimental analysis on the effect of temperature on density and came up with interesting mathematical model to predict the Density of the DES [48]. In general the effect of temperature on density is linear in nature and the density of the solution decreases with the increase in temperature in a very predictable way. Equation 2.9 represents the linear dependence of Density and temperature [37, 49–51].

$$\rho = a + bT \tag{2.9}$$

where
ρ = Density [kg/m^3]
a = Constant [kg/m^3]
b = Constant [kg/$m^3.K$]
T= Temperature [K]

In the equation 2.9 a and b are parameters dependent on the DES. For the current study, table 2.2 provides some values for the density at 398.15 K.

Table 2.2: Literature values for Density of various solvents

Salt (mol equiv.)	HBD (mol equiv)	Density (gm/cm^3)	Reference
ChCl (1)	Ethylene Glycol (2)	1.12	[8]
ChCl (1)	Ethylene Glycol (3)	1.12	[8]
ChCl (1)	MEA (5)	1.07	[11]
ChCl (1)	MEA (6)	1.07	[11]

2.4.3. Viscosity

Typically DES have high viscosity and low conductivity compared to ionic liquids. The origin of this disparity is due to the large size of ions and relatively free volume in ionic liquids. Viscosity in DES is much higher due to the stronger hydrogen bond, causing a lack of free volume. This phenomenon is explained in section 2.4.4. The change in viscosity with temperature is found to correlate with the Arrhenius model for viscosity, represented by equation 2.10 with large values of activation energy for viscous flow [8, 37, 52]. Table 2.3 represents the viscosity data for the chosen DES.

$$\mu = A.e^{\frac{-E_\mu}{RT}} \tag{2.10}$$

Where
μ = Viscosity [mPa.s]

A = Pre-exponential factor[Pa.s]
E_μ = Viscosity activation energy [J/mol]
R = Real Gas constant [J/mol.K]
T = Temperature [K]

2

Equation 2.10 represents the empirical Arrhenius type equation where A and B are adjustable parameters which represent the limits in viscosity at finite temperature and the activation energy of the viscous fluid. It is important to note that the $ln(\mu) = f(1/T)$ is a straight line with slope equal to ln(A) [53]. Bouarab et al. compared various models for viscosities in ionic liquids, in the study it was pointed out that even though DES have similar properties to ILs, DES form complex structures and modeling of the these solvents requires further research [53]. However some research has been done on modeling the variation of viscosity with temperature, models such as Vogel-Fulcher-Tammann (VFT) equation as shown by equation 2.11 where T_o is an adjustable parameter representing temperature at which viscosity becomes infinite, and Litovitz equation as given by equation 2.12 have been studied [52, 53]. The VFT equation though widely used in the literature have been criticised by some authors because of the non-physical divergence of viscosity at finite temperature, resulting in overestimation of viscosity at lower temperature [53]. For this thesis study it is important to maintain consistency in the research and repeatability in results. Various tests on viscosities of DESs have been conducted and Arrhenius-type model is by far the most studies and most accurate model to predict the viscosity of DES with R^2 fit of 0.99 [11, 37, 49, 54].

$$\mu = A.e^{\frac{B}{T-T_o}} \tag{2.11}$$

$$\mu = A'.e^{\frac{B'}{RT^3}} \tag{2.12}$$

The viscosities of DES are in general higher compared organic solvents and hence have limitations in application for heat and mass transfer. The conductivity of the solution is also strongly affected by the viscosity of the solution as high viscosity of the solution affects the mobility of the ions [14].

Table 2.3: Literature values for Viscosity of various DES

salt (mol equiv.)	HBD (mol equiv)	Viscosity (cP)	Reference
ChCl (1)	Ethylene Glycol (2)	36	[8]
ChCl (1)	MEA (5)	48.5	[11]
ChCl (1)	MEA (6)	36.8	[11]

2.4.4. Hole-theory

Novel solutions such as DES, with many advantages, have some limitations, such as increased viscosity and reduced conductivity compared to aqueous solutions. Angell et al. conducted experiments and showed that it is possible to have ionic liquids that could have conductivity and viscosity approaching aqueous solutions [55]. However,

Very few such studies are available to explain the behaviour of viscosity. one of the model that is widely accepted is the Hole Theory proposed by Abbott et al. [38].

The Hole theory assumes that on melting, an ionic meterial contains empty spaces that arise from thermally generated fluctuations in local density, these holes are of random sizes and spread randomly inside the liquid and undergo constant flux[8, 38]. The radius of these holes could be determined by equation 2.13

$$4\pi(r^2) = \frac{3.5kT}{\gamma} \tag{2.13}$$

Where
r = Radius of the hole [m]
T = Temperature [K]
k= Boltzmann constant [kg m^2/s^2.K]
γ = Surface tension [kg/s^2]

The average size of the hole is similar to the dimension of the ions. Hence it is easier for smaller ions to move through the vacant sites, essentially reducing the viscosity. On the other hand, at a lower temperature, the size of the holes will be a smaller couple than with larger molecule size and hence the viscosity increases and can be as high as $10^1 - 10^3$ Pa.S [8].

In order to quantify the viscosity, we assume that the cavities are not formed, but the holes exist and move in the opposite direction to solvent ion/molecule motion. At any given time, the fluid will have a distribution of cavity sizes, and the ions/molecules will only be able to move if the adjacent cavity of a suitable dimension is available. It is hence assumed that at any given moment of time, only a few ions/molecules will be able to move, giving rise to higher viscosity [8, 38]. The probability of finding an ion/molecule-sized hole is higher at higher temperatures than at lower temperatures due to increased mobility. By assuming the limiting factor for viscosity is not the thermodynamics of hole formation but the probability of finding the right size hole, we can justify the reduced viscosity at higher temperatures. In order to reduce viscosity in DES, the ions/molecules should be relatively small, or the liquid should have larger cavities. In order to have a larger cavity size, the surface tension can be reduced by adding a liquid with lower surface tension which will reduce viscosity and increase the conductivity by increasing the whole size [8].

2.4.5. Electrical conductivity

Ohmic losses represent drop in voltage due to the transfer of electrons in the electric circuit and the movement of ions through the electrolyte and membrane. Ohmic losses in the electrochemical cell is due to the electrodes and the current collector, along with the movement of ions in the electrolyte. A solution where it is easier for ions to move will have less Ohmic losses and vice versa. In order to find a suitable solution that is a good electrolyte, it is important for the solution to have higher conductivity in order to reduce Ohmic losses. Abbott et al. explained in the hole

theory how conductivity is directly related to viscosity. As discussed in section 2.4.4, the electrical conductivity similar to viscosity is not limited by the thermodynamics of hole formation but by the probability of finding a hole [8]. With an increase in temperature, the viscosity decreases as the hole size increases due to a reduction in surface tension; this increases the ion mobility hence increasing the conductivity of the solution. The electronic conductivity decreases for increasing temperature in most of the conductive materials, whereas higher temperatures increase the ionic conductivity due to a reduction in viscosity. Also, adding liquids with lower surface tension will also increase conductivity. As discussed before KCl is a standard calibration solution used in most of the electronically measurements and has a relatively high conductivity of about 11.88 mS/cm at room 293.15 K, This thesis will aim to find a solution with conductivity as close to KCl solution as possible.

Electrical conductivity for ChCl:EG solution is known to be 7.61 mS/cm [8], the value for other solvents is not known which will be a novelty for this research as it has not been done before.

In section 2.4.4 it was discussed that adding water to the solution increases conductivity. The reason for this is that adding water reduces viscosity in the liquid allowing ions to move freely. Reaction 2.14 represents the reduction reaction of CO_2 in the electrolyzer. It was observed that adding more water in the solution reduces the formation of CO, and reaction 2.15 is favoured. This is not good for the CO_2 reduction process, the details of which are beyond the scope of this research. In order to remove water, an organic solvent with low surface tension is used. As described in the equation 2.13 reducing the surface tension of the fluid will increase the hole radius and reduce viscosity and increase conductivity.

$$CO_2 \xrightarrow[e^-]{H^+} CO^- \tag{2.14}$$

$$H_2O \xrightarrow[e^-]{H^+} H_2 \tag{2.15}$$

2.5. Conclusion

Based on the information gathered from the literature survey the following information can be gathered.

- Choline Chloride Ethylene glycol has shown some promising results for high pressure CO_2 absorption, and higher conductivity with low viscosity makes it an ideal candidate for consideration.
- Amines have shown very high potential in CO_2 absorption technology and DES such as ChCl:MEA in various molar ratios could be tested for potential solutions for CO_2 absorption.
- Amino Methyl Propanol (AMP) could potentially be an interesting amine to consider as it is a sterically hindered primary amine which results in formation of bicarbonates instead of carbamates which could be a good alternative because of low heat of desorption.

- Two film theory explains the limitation on diffusion and mass transfer at the gas liquid interface
- From the hole theory shows the limiting factor on viscosity and explains how formation of carbamates increase viscosity and reduce conductivity
- The formation of strong hydrogen bonds between choline chloride and HBDs generates a decrease in free volume to play an essential part in the observed change in density. It is also observed that at a fixed temperature, the density decreases with a higher molecular weight of the HBD as a result of the observed decrease of the density of pure HBDs.
- If the viscosity of the selected sorbents is relatively high, it plays as a limiting factor for a good mass transfer. In general, the viscosity decreases markedly with an increase in temperature. At a fixed temperature, the viscosity increases when choline chloride (HBA) is added to the mixture. The increase can be mostly attributed to the formation of hydrogen bonds, which results in loss of molecular mobility.
- The effect of water on the viscosity of pure and CO_2 loaded sample needs to be quantified, and viscosities for different water and CO_2 concentration should be measured.
- Ohmic losses are higher in solvents with low conductivity, improving conductivity is crucial for electrochemical conversion process. Conductivity is dependent on viscosity as increasing viscosity leads to reduction in conductivity. Increasing temperature reduces viscosity and increases conductivity.
- Electrochemical reduction of CO2 in the aqueous electrolyte has been a challenging subject since the competing hydrogen evolution reaction (HER) takes place at very close potential windows to CO2RR reaction. Therefore, there is a need to investigate the CO2RR in other solvents rather than water

Table 2.4 depicts the chosen DES. The next section deals with the experiment setup that need to be carried out and further sections deal with the results and conclusions drawn from this thesis study.

Table 2.4: Selected DES for this thesis study

Salt	HBD	Molar Ratio
Choline Chloride	Ethylene Glycol	1:2
Choline Chloride	Ethylene Glycol	1:3
Choline Chloride	Ethylene Glycol	1:4
Choline Chloride	Monoethanol amine	1:5
Choline Chloride	Monoethanol amine	1:6
Choline Chloride	Aminomethyl propanol	1:6

3

Experimental setup

This chapter deals with the experimental setup and sample preparation. Based on the observation made in the section 2.5, experiments have been planned and the results for these experiments will be discussed in Chapter 4.

3.1. Preparation of solvents

It is important to first establish the method used to prepare the solvents. The method used in preparing the solvents is similar to the one performed by Abbott et al. [35]. The key difference is the amount of water added to the solution. Abbott et al. kept negligible amount of water in DES, this is achieved by drying the choline chloride and using high purity of individual compounds [8, 35]. In the case of this thesis, study the purity of individual compounds was higher than 98% but it was observed that any solution with no water would develop crystals as shown in figure 3.1. This crystallisation was observed in ChCl:EG (1:2), ChCl:MEA(1:5) and ChCl:MEA(1:6). After Various iterations and changing the water concentration of the solution, it was found that 3%wt of solution, concentration of water gives a solution and did not develop crystals and has a longer shelf life. Figure 3.1 shows the schematic diagram for sample preparation. Details for the sample preparation and the instruments used can be found in appendix A along with figure A.1

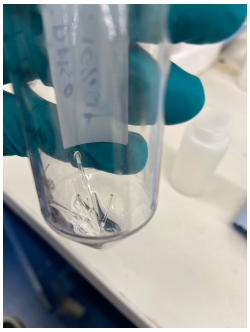

(a) Crystals in ChCl:EG(1:2)

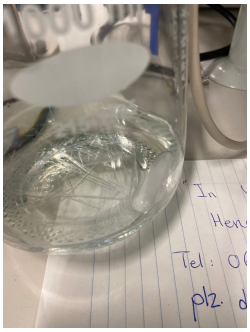

(b) Crystals in ChCl:MEA(1:5)

Figure 3.1: Crystal formation without water in the solution

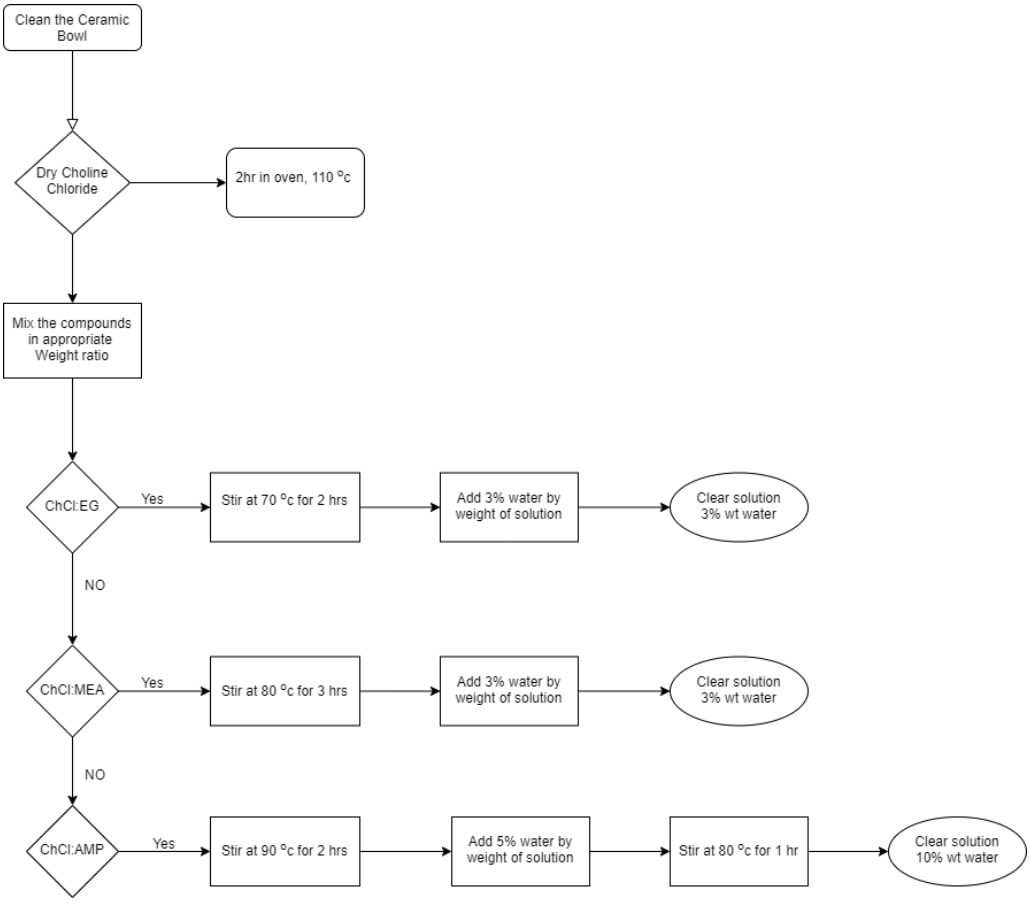

Figure 3.2: Schematic representation of Sample preparation

3.1.1. Adding organic solvents

As discussed in section 2.4.5, organic solvents have been added to DES in order to reduce the water content in DES. Higher water content in DES is not desired as it interferes during the CO_2 reduction process. In section 2.4.5 it was discussed that increased viscosity will reduce electrical conductivity. To reduce viscosity in amine based DES, an organic solvent with low surface tension was added. In the case of this study, EG solution was added to amine based DES.For example, ChCl:MEA (1:6) has about 11 moles of MEA per liter of solution, similar amount was observed for AMP. In order to observe the effect of different quantities of organic solvent in the DES, the molarity of MEA/AMP was varied in ChCl:EG solution. To prepare the solution, a known amount of ChCl:EG solution was taken and three different morality (3, 6 and 9) of MEA/AMP were added. The details of the mixtures and exact molarity of amines can be found in Appendix A in the tables A.1 and A.2

3.2. CO_2 loading setup

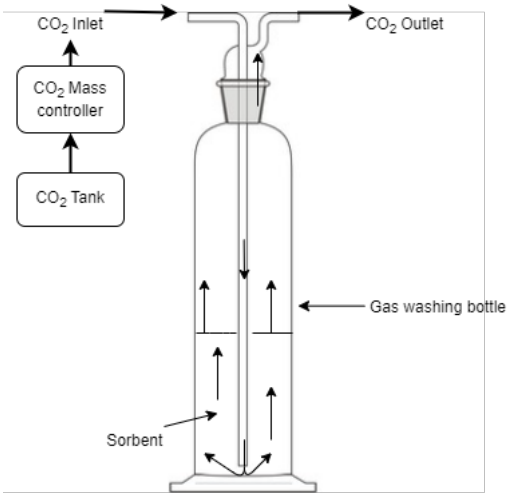

Figure 3.3: Schematic diagram of CO_2 loading setup

Figure 3.3 shows the schematic diagram of the setup used for loading CO_2 in the sorbent. A mass flow controller is attached to the outlet of CO_2 tank. The pressure is set to 2 bar ,the mass flow controller is then attached to the inlet of gas washing bottle. About 100-150 ml of pure DES solution is put inside the bottle. CO_2 is then bubbled in the solution for about 30-40 minutes depending on the solution. This time for loading is determined by multiple tests conducted in order to find the ideal loading capacity to test viscosity and conductivity. For instance, a very heavy loaded sample will be too viscous for the rheometer to measure viscosity along with very low conductivity which cannot be measured in the conductivity meter. The outlet of the gas washing bottle is open to the vents to remove the excess undissolved

gas. Once the CO_2 loading is completed, the bottle is washed, dried, and made ready for the new sample to be loaded. The amount of CO_2 loaded in the sample is measured using barium chloride titration. To make different concentration of CO_2 in a solution, a master batch of 300 ml pure DES was loaded with CO_2. This master batch is then diluted by adding pure DES in the solution. This dilution process is discussed in section 3.2.2.

3.2.1. Barium chloride titration

CO_2 concentration was determined by barium chloride titration method. The test uses the reaction 3.3, which is the overall reaction derived for of stage reaction 3.1 and 3.2. The $BaCO_3$ formed in the reaction 3.3 is a white precipitate and does not dissolve in water or organic solvent. This precipitate forms in 1:1 ratio with the moles of CO_2 present in the solution hence, measuring the amount of $BaCO_3$ in the solution will give the amount of CO_2 present in the solution.

There are various methods to determine the quantity of $BaCO_3$ precipitate. One way is to filter the precipitate and wash with water to remove the undissolved NaOH then dry and weigh the precipitate. This is a tedious method which takes about 1-2 days as the precipitate should be completely dry. This method also results in some filtrate losses. Another method is to titrate the solution using HCl, the tritration follows the reaction 3.4. Pérez-Gallent et al. performed barium chloride titration to determine the CO_2 absorption in AMP where in the CO_2 rich solution was treated with NaOh and $BaCl_2$. The precipitate $BaCO_3$ titrated using HCl until a clear solution is obtained [56]. Figure 3.5 shows the procedure of the titration. The detailed procedure is as follows:

1. 25ml 0.5M solution of $BaCl_2$ and 25ml 0.5M solution of NaOH are mixed with a known amount of CO_2 loaded sample and this mixture is stirred at 70 ^oC for 3 hr.

2. The solution is allowed to cool down to the room temperature. While stirring, white precipitate is observed.

3. Phenolphthalein is added. The solution turns to pink colour as shown in figure 3.4a. This solution is then titrated using 1M HCl solution.

4. After titration, the first end point is reached when the solution becomes transparent again with a white precipitate as shown in figure 3.4b. This indicates that all the bases (excess NaOH) have been neutralised.

5. At this stage, Methyl Orange indicator is added. The solution turns to a yellowish colour as shown in figure 3.4c.

6. Further titrating with HCl solution starts to dissolve the precipitate present in the solution and the final end point is reached when the solution has no precipitate. Now the solution has a lighter shade of orange colour as shown in figure 3.4d.

The amount of HCl used in step 6 is measured and the moles of $BaCO_3$ can be calculated. Since $BaCO_3$ and CO_3^{-2} react in 1:1 ratio, the moles of CO_2 in the sample can be calculated.

$$2\,NaOH_{(aq)} + CO_{2(aq)} \longrightarrow Na_2CO_{3(aq)} + H_2O_{(aq)} \tag{3.1}$$

$$Na_2CO_{3(aq)} + BaCl_{2(aq)} \longrightarrow 2\,NaCl_{(aq)} + BaCO_{3(s)} \tag{3.2}$$

$$Na^{+}_{(aq)} + CO^{-2}_{3(aq)} + BaCl_{2(aq)} \longrightarrow 2\,NaCl_{aq} + BaCO_{3s} \tag{3.3}$$

$$BaCO_{3(s)} + 2\,HCl_{(aq)} \longrightarrow BaCl_{2(aq)} + CO_{2(g)} + H_2O_{(aq)} \tag{3.4}$$

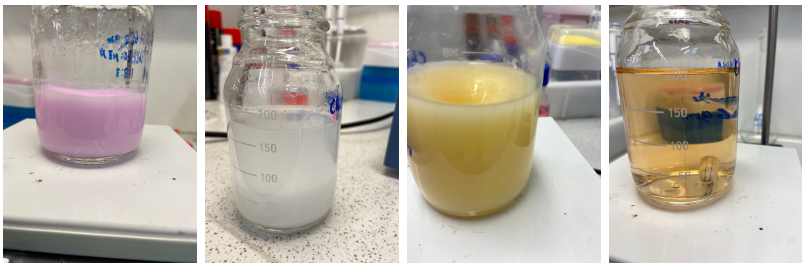

(a) Adding phenolphthalein (b) Phenolphthalein end point (c) Adding methyl orange (d) Methyl orange end point

Figure 3.4: Baroum chloride titration end points

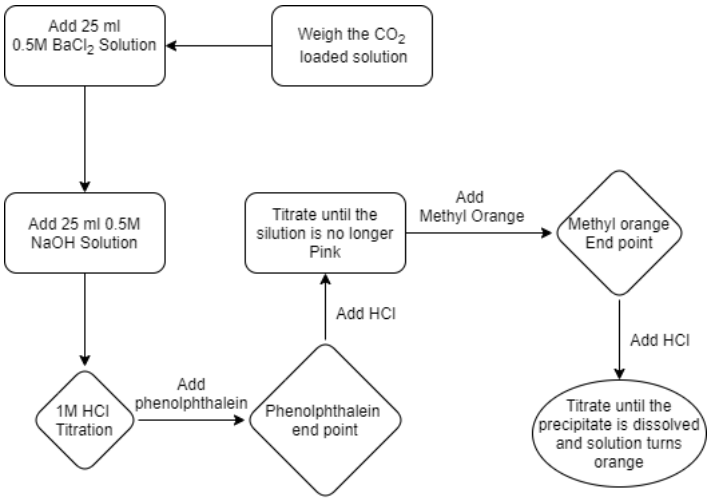

Figure 3.5: Schematic description of barium chloride titration

3.2.2. Dilution

Once the amount of CO_2 in the sample is determined, we proceed to dilute the solution from the batch solution. The diluted solution is used to measure physical properties at different concentrations of CO_2 and H_2O.

The master batch with high CO_2 concentration is diluted with adding pure DES solution and water. Table 3.1 shows the values for the CO_2 in various diluted sample and further these solutions are diluted by adding water represented by table 3.2. The same procedure was applied to ChCl:AMP solution. Table A.3 and table A.4 can be found in Appendix A.

Table 3.1: Dilution of CO_2 loaded ChCl:MEA(1:6) samples by adding pure DES

Co_2 loaded sample (g)	Pure sample (g)	Co_2 in the sample (wt% of solution)
60.04	163.44	2.22
120.05	180.06	3.31
189.05	126.08	4.97
298.00	0.00	8.28

Table 3.2: dilution of CO_2 loaded ChCl:MEA (1:6) sample with H_2O

CO_2 concentration (%wt of solution)	Weight of sample (g)	Water added (g)	Water concentration (%wt of solution)
2.22	87.00	0.000	2.92
	61.90	4.87	10.02
	54.19	12.15	20.69
	46.68	18.35	30.31
3.31	88.00	0.00	2.92
	77.11	6.02	9.94
	73.69	15.62	19.90
	62.57	24.00	29.83
4.96	85.00	0.00	2.92
	83.08	6.64	10.11
	76.23	16.17	19.90
	68.63	26.27	29.79
0	38.08	2.97	9.95
	35.59	7.59	19.99
	31.51	12.15	29.93

3.3. Fourier-Transform Infrared Spectroscopy (FTIR)

Figure 3.6: Nicolet iS50 FT-IR machine

Figure 3.6 shows the setup for Fourier-Transform Infrared Spectroscopy (FTIR). This equipment is used to identify various bonds in the solvent and how and when new bonds are formed resulting in the formation of different compounds. The machine sends infrared radiation of about 10,000 to 100 cm^{-1} through the sample. Some of the radiations are absorbed and some are passed through. The absorbed radiation by molecules is converted into rotation and/or vibration energy. The resulting signal received at the detector is presented as an absorption spectrum. For this specific machine the wavenumbers in the spectrum are form 4000 cm^{-1} to 400 cm^{-1}. The spectrum generated is a series function of absorbed energy. This particular machine uses a zinc selenide crystal which provides more durability at the cost of small error. For higher resolution, germanium crystal could be used. This experimental setup measures 16 iteration per sample and the resolution of 2 cm^{-1}.

3.4. Density measurement

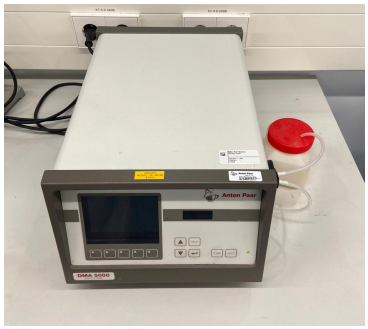

Figure 3.7: Anton Paar DMA 5000 density meter

Figure 3.7 shows the density meter used in this work. This machine has a U bent transparent tube. The sample is injected in the tube. The tube is then vibrated.

Each vibration frequency is calibrated to a density value. The frequency of the vibration is then compared to the base calibration reading. The difference in reading gives the density of the sample. This machine can measure the density at different temperature ranging from 0-100 ^{o}C with a least count of 10^{-6} g/cm^3. The results could be found in appendix B.

3.5. Viscosity measurement

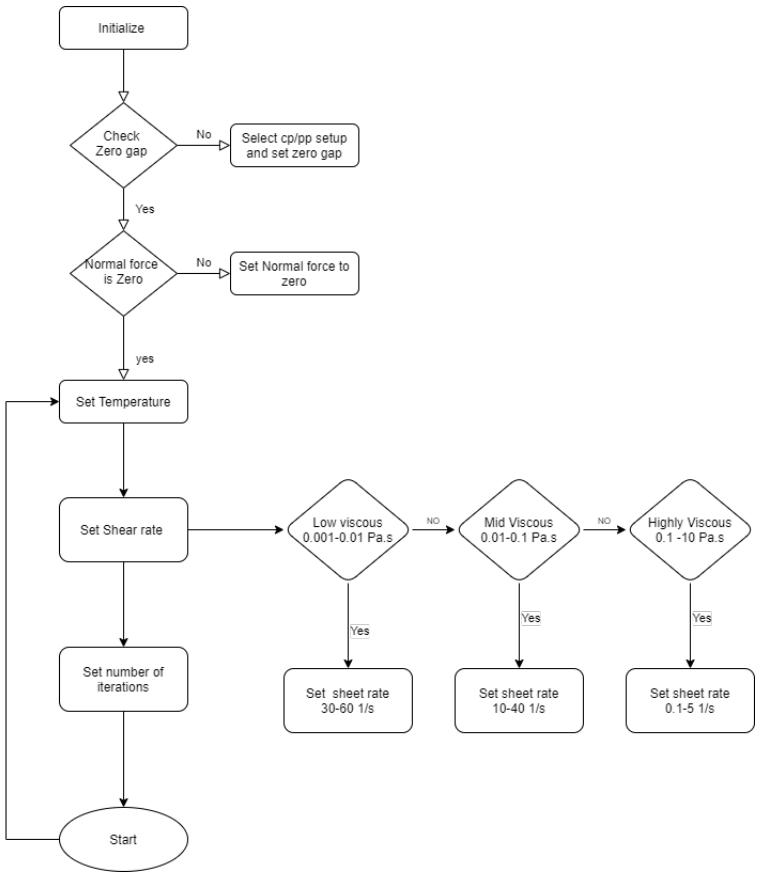

Figure 3.8: Schematic diagram of viscosity measurement

Figure 3.8 shows the procedure for measuring viscosity. The machine used in this work (figure 3.9) measures shear stress and using the equation 3.5, the viscosity is calculated. The procedure of this instrument is as follows:

- The suspended arm of known flat plate area as shown in the figure 3.9 is lowered to a gap of 1mm from the metal plate. This is the y variable in the equation 3.5 and A is the area of the plate in contact with the fluid.

- The suspended arm is rotating about an air bearing and is connected to a sensor which measures the shear stress in the suspended arm when it is in motion. This sensor gives the F value for the equation 3.5.

- Shear rate is set using the Anton Paar software in the machine. Once the machine starts to rotate at the specified shear rate, the value for $\frac{u}{y}$ in the equation 3.5 is obtained.

- The value of these variables is put in the equation by the software and the viscosity is calculated.

In order to get accurate measurements, 21 iterations were taken with varying the shear rate. As represented in the table 3.3, the shear rate was varied from 20-50 and 21 readings were noted. It is important to take several readings to reduce errors. In this measurement, the average error percentage was less than 3%.

$$\mu = \frac{F}{A}.\frac{y}{u} \tag{3.5}$$

where,
μ : Viscosity [Pa.s]
A : Area of the plate $[m^2]$
F: Shear stress [Pa]
$\frac{u}{y}$: Shear rate $[s^{-1}]$

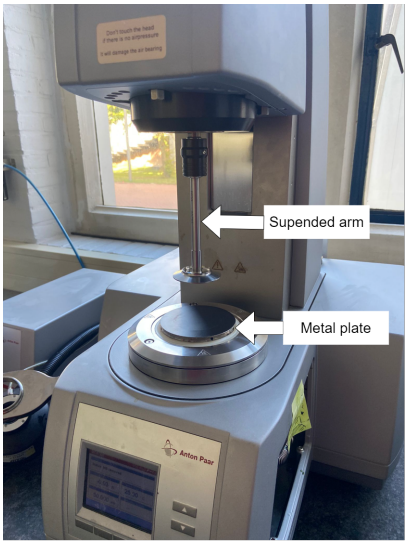

Figure 3.9: Anton Paar rheometer

Table 3.3: Viscosity measurement at 313.15 K for ChCl:EG(1:3) solution

Point No.	Shear rate (s^{-1})	Shear stress (Pa)	Viscosity (mPa.s)	Error (%)
1	20.00	0.30	14.96	2.15
2	21.50	0.32	14.81	1.14
3	23.00	0.34	14.70	0.35
4	24.50	0.36	14.64	-0.02
5	26.00	0.38	14.62	-0.15
6	27.50	0.40	14.63	-0.06
7	29.00	0.43	14.67	0.16
8	30.50	0.45	14.72	0.52
9	32.00	0.47	14.69	0.33
10	33.50	0.49	14.58	-0.44
11	35.00	0.51	14.61	-0.24
12	36.50	0.54	14.66	0.09
13	38.00	0.55	14.57	-0.49
14	39.50	0.58	14.64	-0.02
15	41.00	0.60	14.59	-0.38
16	42.50	0.62	14.60	-0.27
17	44.00	0.64	14.61	-0.26
18	45.50	0.66	14.56	-0.55
19	47.00	0.68	14.55	-0.64
20	48.50	0.71	14.56	-0.59
21	50.00	0.73	14.55	-0.64

3.6. Conductivity measurement

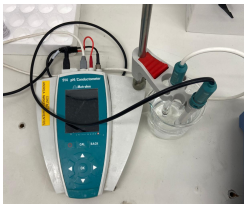

Figure 3.10: Metrohm - pH/conductometer

Figure 3.10 shows the conductivity meter. It can measure conductivity as low as 1 $\mu S/cm$ as high as 100 mS/cm. This thesis study is used to measure conductivity at room temperature 294-296 K. The machine is simple to use. It is first calibrated using a standard KCl solution, the conductivity of the standard solution is calibrated at 298.15 K, and the machine is calibrated. Once calibrated, it measures the conductivity of the solvent based on the potential difference applied. The value obtained is compared to the calibrated value and gives conductivity.

*Note: The machine after each measurement needs to be washed, while washing with water the electrode which is inside the outer cover cannot be properly dried hence, there can be some discrepancies in the experimental values. The amount of water is small which results in error between each reading to be about 2-5% but not more.

4

Results and Discussion

This chapter deals with the experimental results obtained. The aim of the thesis is to find a solvent suitable for CO_2 absorption and a suitable electrolyte for electrochemical conversion process. The experiments were conducted to determine the physico-chemical properties of the solution in order to determine the limiting factors of CO_2 absorption and electrochemical conversion. These results were later used to find the most suitable solution for the process.

4.1. Pure solvents

4.1.1. Viscosity

Figure 4.1 represents viscosities for the selected DES over four different temperatures ranging 303.15 and 333.15 K. As discussed in section 2.4.3, viscosity of DES follow Arrhenius equation, as shown in equation 2.10. Table 4.1 compares the coefficients for the Arrhenius equations obtained from experiments and literature study.

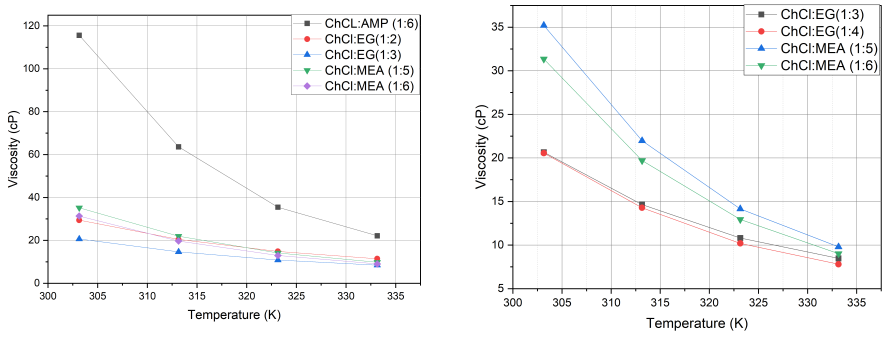

(a) Viscosity comparison between selected DES (b) Viscosity comparison between DES

Figure 4.1: Viscosity vs Temperature for selected DES

From Figure 4.1 it can also be observed that the viscosity for ChCl:AMP (1:6) solution is much higher compared to other solvents. Comparing the values of the activation energy for the the solvents, AMP has the highest activation energy in all of the solvents. In the selected solvent,the order of molecular size is AMP>MEA>EG. AMP solvent is the most bulkiest organic molecule in the selected solvents hence has the largest size. As discussed in section 2.4.4, viscosity is dependent on the void size and bigger molecules will have less mobility through voids hence, higher viscosity. Similarly the activation energy for MEA DES is higher than that of EG DES and hence have higher viscosity.

Table 4.1: Comparing Arrhenius coefficients obtained from literature and experimental values with the regression coefficient

Solvent	A (mP.s)		B (k)		R^2 (Experiment)
	Experimental	Literature	Experimental	Literature	
ChCl:EG (1:2)	$8 * 10^{-4}$	$1.5 * 10^{-3}$	-3187.5	-2978.9	0.99
ChCl:EG (1:3)	$1 * 10^{-3}$	N/A	-3009.5	N/A	0.99
ChCl:MEA (1:5)	$2 * 10^{-5}$	$6 * 10^{-5}$	-4324.2	-4071.7	0.99
ChCl:MEA (1:6)	$3 * 10^{-5}$	$1.8 * 10^{-4}$	-4204.2	-4204.2	0.99
ChCl:AMP (1:6)	$1 * 10^{-6}$	N/A	-5606.0	N/A	0.99

4.1.2. Electrical conductivity

Figure 4.2 shows the value of electrical conductivity measured for the selected DES at 294.5 K. Comparing the conductivity, ChCl:EG(1:3) has the highest value. As discussed in section 2.4.4, the electrical conductivity has a high dependence on viscosity as the mobility of charge through the solution is limited by the viscosity of the solution. It can be clearly seen that the solvent with the least viscosity (ChCl:EG(1:3)) has the highest conductivity and the solvent with the highest viscosity (ChCl:AMP(1:6)) has the lowest conductivity.

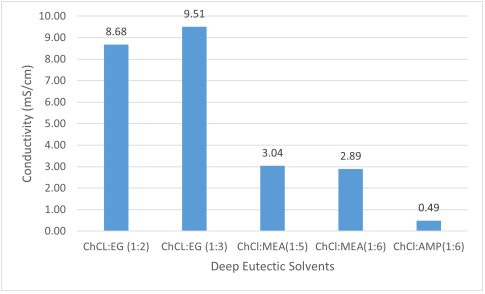

Figure 4.2: Electrical conductivity of selected DES

4.2. Effect of water

The effect of water is quite predominant as discussed in the section 2.4.4. Abbott et al mentioned that adding water will increase conductivity and reduce viscosity

[8]. This section deals with the effect of adding different concentrations of water to the DES and seeing the effect of water on physical parameters.

4.2.1. Viscosity

Viscosity is an important parameter for absorbing CO_2 in a solvent. As discussed in the section 2.3.3, the absorption of CO_2 in the solution is limited by the diffusion. As the viscosity increases, the diffusion of gas in the solution decreases hence, limiting the CO_2 absorption capacity of the solvent. As discussed before, viscosity of the solvent could be decreased by adding water and from figures 4.3 - 4.5 it can be seen that the adding water to the solution reduces viscosity.

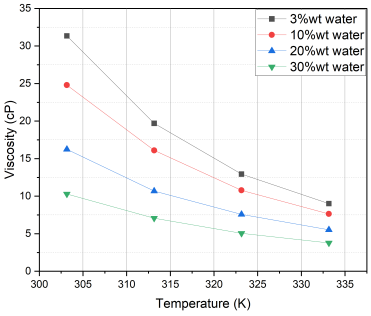

(a) Viscosity vs temperature with different water concentration

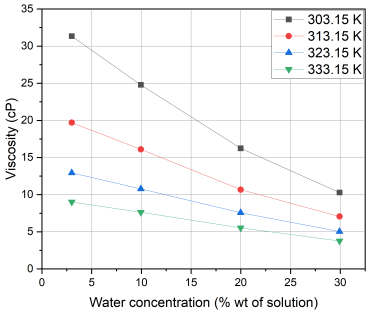

(b) Isothermal comparison of viscosity with different water concentration

Figure 4.3: Effect of water concentration on viscosity for pure ChCl:MEA (1:6) solution

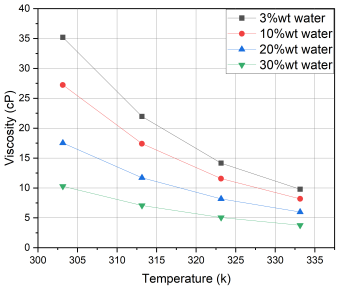

(a) Viscosity vs temperature curve with different water concentration

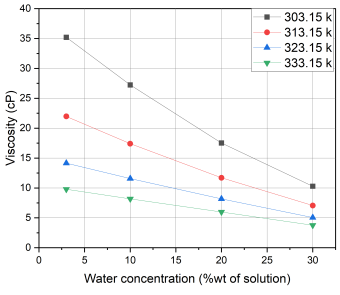

(b) Isothermal comparison of Viscosity with different water concentration

Figure 4.4: Effect of water concentration on viscosity for pure ChCl:MEA (1:5) solution

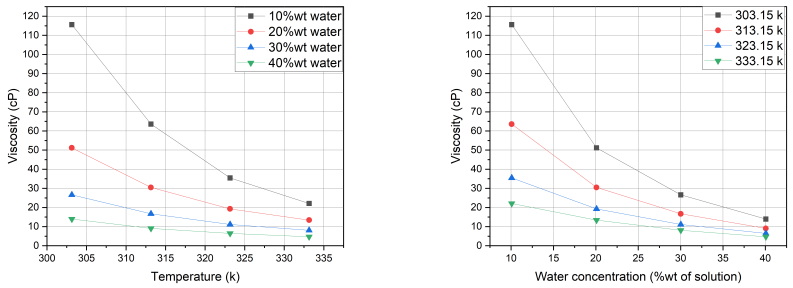

(a) Viscosity vs Temperature curve with different water concentration

(b) Isothermal comparison of Viscosity at different water concentration

Figure 4.5: Effect of water concentration on viscosity for pure ChCl:AMP (1:6) solution

Figure 4.3a, shows the variation for viscosity in ChCl:MEA (1:6) solution over a temperature range with different concentrations of water in the solution. It follows the Arrhenius equation. Similar effect was observed for ChCl:MEA (1:5) and for ChCl:AMP (1:6) solutions as shown by figure 4.4a and figure 4.5a respectively. It is evident from the results that ChCl:MEA (1:6) has the least viscosity among the amine-based solvents at about 31.35 cP at 303.15 K. ChCl:AMP (1:6) solution has the highest viscosity of 115.6 cP.

Abbott et al. explained the viscosity of DES using the hole theory as discussed in section 2.4.4. The theory states, the viscosity of a DES is determined by the size of the hole and the probability of the moving molecule to find a hole of appropriate size [8, 38]. From the equation 2.13, it was also theorised that adding a solvent with lower surface tension will reduce the viscosity of the solvent by increasing the hole size. However, it is observed that adding water will reduce the viscosity even when the surface tension of water is much higher than DES. The surface tension of ChCl:MEA (1:6) solution is 48.21 mN/m at 298.15 K [11]. The surface tension of water is about 70.4 at 298.15 K. Even though the surface tension of water is much higher than ChCl:MEA (1:6). From figure 4.3b, it can be observed that the viscosity of ChCl:MEA (1:6) solution decreases with increasing the water content.

Garcia et al. conducted a theoretical study on choline chloride-based DES with glycerol, and malonic acid [57]. They analysed the geometry of the DESs as well as characterised the hydrogen network structure. the study was performed to understand the molecular structure and how the addition of H_2O and CO_2 affects the molecular structure of the solution. Based on the results, it was observed that adding H_2O in the DES increases the OH bonding in the solution. The bond length between the Cl^- ion and hydrogen molecule increases because of the oxygen molecule from water as shown in figure 4.6. This change in the bond length results in the stretching of OH bonds. This increases the hole size and improves molecular/ionic mobility in the solution hence reducing viscosity. Based on the FTIR results, there is an increase in OH bonds abundance in the solution when the concentration of water is increased. The addition of water changes the intensity but does not alter

the wavenumber of the OH bond.

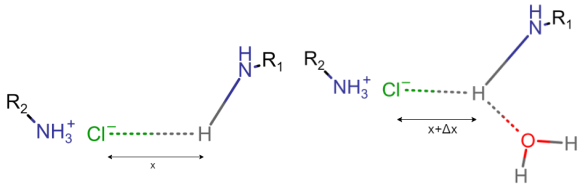

(a) Hydrogen bonding in pure DES

(b) Hydrogen bonding in presence of water

Figure 4.6: Hydrogen bonding length in pure solvent and in presence of water

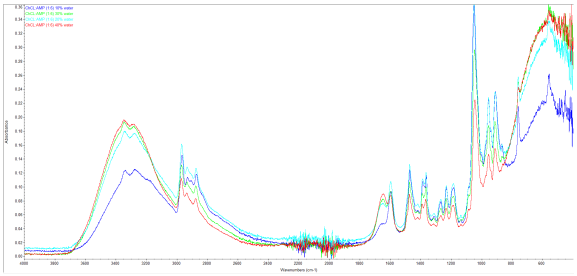

(a) FTIR spectrum for ChCl:AMP(1:6) solution with different water content

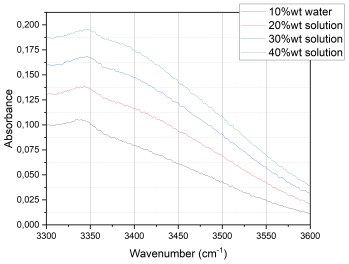

(b) Zoomed in FTIR spectrum for pure ChCl:AMP(1:6) solution

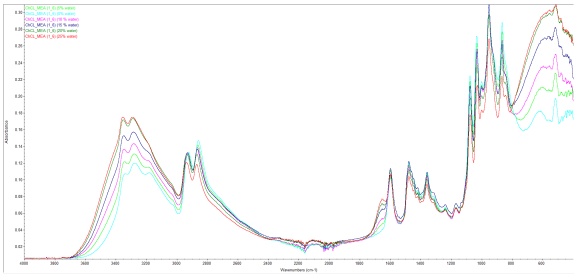

(c) FTIR spectrum for pure ChCl:MEA(1:6) solution with different water content

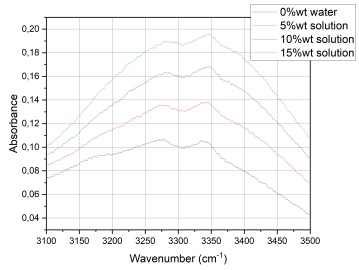

(d) Zoomed in FTIR spectrum for ChCl:MEA(1:6) solution

Figure 4.7: FTIR spectrum for amine based DES with different water content

Figure 4.7, shows the FTIR spectrum for ChCl:MEA (1:6) and ChCl:AMP (1:6) solutions with different water content. In amine-based solvents, the OH bond has a wavenumber of 3355 cm^{-1} [58]. From the figure 4.7b, the peak at 3352 cm^{-1} is rising with increasing water concentration in the DES. Comparing the rise in the

water concentration to viscosity drop-in figure 4.5b, a significant drop in viscosity can be observed when water concentration goes from 10%wt of solution to 20%wt of solution. This drop can be compared to a rise as seen in figure 4.7b at wavenumber 3353 cm^{-1} when the water concentration rises from 10%wt of solution to 20%wt of solution. A similar trend is observed in ChCl:MEA(1:6) solution. From figure 4.7d, it can be seen that an increase in OH bond corresponding to wavenumber 3352.3 cm^{-1}.

4.2.2. Electrical conductivity

Electrical conductivity is dependent on viscosity, and as the viscosity decreases, the electrical conductivity increases. As discussed in section 2.4.5, the mobility of ions in the solution is dependent on the hole sizes and the probability of finding voids to move through. From figure 4.8, it can be observed that the change in viscosity is inversely related to the change in conductivity. In figure 4.8a, it can be seen that for ChCl:MEA(1:6), viscosity drops from 31.35 to 10.29 cP when the water concentration changes from 3% to 30%wt of solution, and conductivity changes from 2.89 to 8.16 mS/cm. Comparing ChCl:AMP (1:6) and ChCl:MEA (1:6) solutions at 30%wt water solution, the viscosities are low, but the electrical conductivity for ChCl:AMP (1:6) solution as seen from figure 4.8b is very low. The highest conductivity obtained by ChCl:AMP (1:6) is at water concentration of 40%wt of solution of 4.55 mS/cm compared to 8.16 mS/cm obtained by ChCl:MEA(1:6) at lower water concentration. As mentioned in the section 2.4.5, a lower concentration of water is desired for the process.

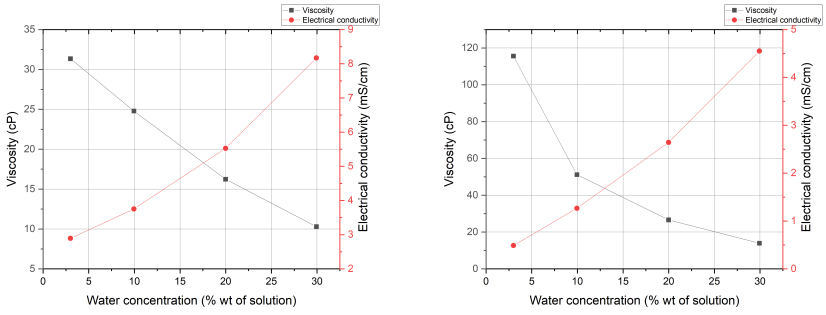

(a) Electrical conductivity and viscosity vs water content for for ChCl:MEA(1:6) solution

(b) Electrical conductivity and viscosity vs water content for ChCl:AMP(1:6) solution

Figure 4.8: Comparing viscosity and conductivity at different water content for different amine based solvents

4.3. Effect of CO_2

As discussed in the previous section, addition of water has a significant effect on viscosity and electrical conductivity. This section deals with the effect of CO_2 absorption in amine based DES.

4.3.1. CO_2 absorption in MEA solution

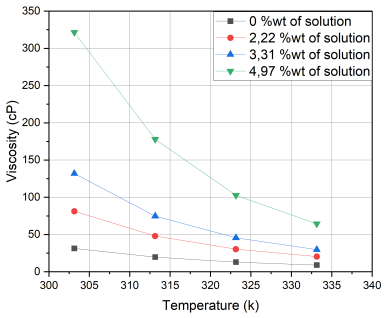

(a) Viscosity vs temperature for different concentration of CO_2

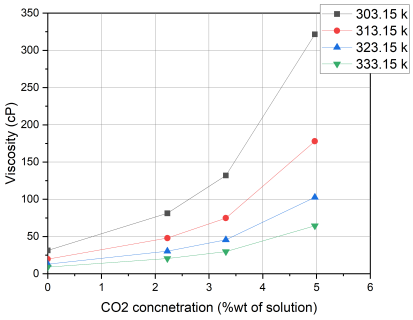

(b) Isothermal comparison of change in viscosity with different concentrations of CO_2

Figure 4.9: Comparing change in viscosity at different temperature and different concentration of CO_2 for ChCl:MEA(1:6) solution

CO_2 absorption in the solution was carried out using the method described in section 3.3. The amount of CO_2 absorbed is determined by barium chloride titration method as discussed in section 3.2.1. CO_2 reacts with MEA and forms carbamates as shown by reaction 2.2. Carbamate formation increases the molecule size, but the hole/void size remains the same resulting in higher viscosity. Figure 4.9 shows the variation of viscosity with different concentration of CO_2 in ChCl:MEA (1:6) solution. It can be clearly seen from figure 4.9b that as the concentration of CO_2 absorbed in the solution increases, the viscosity of the solution also increases. From figure 4.9a it can be seen that viscosity of the CO_2 rich solvent also follows the Arrhenius equation represented by 2.10.

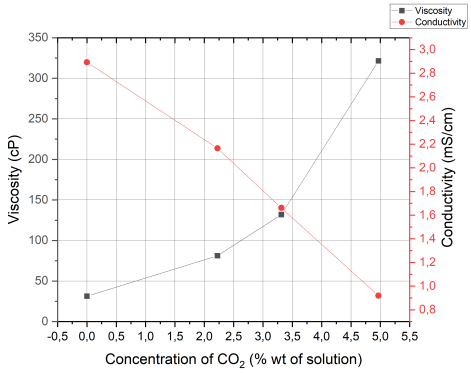

Figure 4.10: Comparing change in electrical conductivity and viscosity with CO_2 concentration in ChCl:MEA(1:6) solution

As discussed previously, electrical conductivity is highly dependent on the viscosity of the solution. From figure 4.10 it can be seen that as the concentration of CO_2 in the solution increases, the viscosity of the solution also increases and hence the conductivity of the solution decreases. There is a clear correlation between the viscosity and conductivity of the solution.

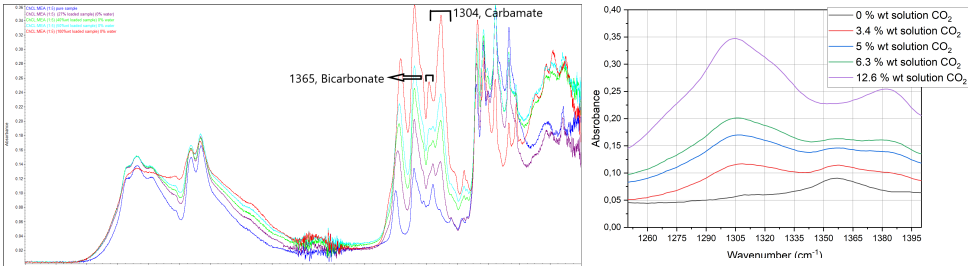

(a) FTIR spectrum for ChCl:MEA (1:6) solution with different concentraion of CO_2

(b) Zoomed FTIR spectrum for different concentration of CO_2 in ChCl:MEA(1:6) solution

Figure 4.11: FIRT plot for different concentration of CO_2 for ChCl:MEA(1:5) solution

Figure 4.11 shows the FTIR spectrum for ChCl:MEA (1:6) solution with different concentration of CO_2. As discussed previously MEA reacts with CO_2 to form carbamates as shown by reaction 2.2. In the FTIR spectrum , the carbamate bond peak is observed at 1322 [59]. In ChCl:MEA DES the peak was observed at 1307, as shown in figure 4.11b the peak at 1307 increases with as the concentration of CO_2 increases. It was also observed that at higher concentration of CO_2 in the solution, bicarbonate formation was observed. This bicarbonate formation is represented by the peak observed at 1365-1385 wavenumber in figure 4.11b. It is important to note that this bicarbonate peak was only observed at high loading of CO_2.

4.3.2. CO_2 absorption in AMP solution

AMP, as discussed before, is a sterically hindered amine which on reaction with CO_2 forms unstable AMP-carbamates and in the presence of water, these carbamates dissolve and become bicarbonates as shown by reaction 2.3. When CO_2 is loaded in the ChCl:AMP (1:6) solution, the CO_2 reacts with AMP and forms a precipitate which is are the unstable AMP-carbamates. Svensson et al. also observed similar precipitate formation during the study involving AMP in an organic solvent,N-methyl-2-pyrrolidone or triethylene glycol dimethyl ether [60]. Figure 4.12 shows the precipitate formed after reaction with CO_2. The formation of the precipitate results in a two-phase solution which severely limits the CO_2 absorption capacity of the solvent. A higher amount of CO_2 could be absorbed by the solvent at a higher water concentration as the addition of water to the solvent converts the carbamates into bicarbonates. Due to the limitation of CO_2 absorption due to the formation of two-phase solution, only a small amount of CO_2 could be absorbed in the solution, and the change in viscosity could not be noted because of high amount of water

present in the solution. More information regarding absorption of CO_2 in AMP could be found in Appendix B.2

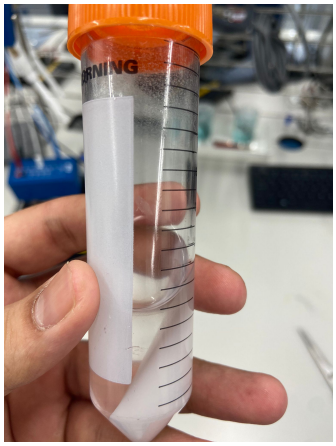

Figure 4.12: ChCl:AMP (1:6) solvent with precipitate after reacting with CO_2

4.4. Mathematical fit for physical parameters

This section deals with developing a mathematical fit for the physical parameters and determining an equation for the same. The parameters in the equation will be a function of CO_2 and H_2O concentrations in the solvent. It is important to establish the interdependence between concentrations of CO_2 and H_2O as it is observed they have a significant effect on viscosity and electrical conductivity of the solutions.

4.4.1. Viscosity

The idea behind making a mathematical fit it to obtain an equation like the Arrhenius equation as shown in 4.1. In the equation viscosity is dependent on coefficients A_m and B_m which are variables dependent on the concentration of CO_2 and H_2O in the solvent. The coefficients were determined for both ChCl:MEA(1:6) and ChCl:AMP(1:6) solutions.

$$\mu_{(CO_2,H_2O,T)} = A_{m(CO_2,H_2O)} exp^{\frac{-B_{m(CO_2,H_2O)}}{T}} \tag{4.1}$$

Table 4.2: Experimental values for viscosity of ChCl:MEA(1:6) solution with different concentration of H_2O and CO_2

Concentration		Viscosity (Temperature) (cP)			
H_2O (wt% of solution)	CO_2 (wt% of solution)	303.15 K	313.15 K	323.15 K	333.15 K
3.00	0.00	31.35	19.70	12.94	9.01
9.95	0.00	24.79	16.10	10.78	7.64
19.99	0.00	16.24	10.68	7.57	5.53
29.93	0.00	10.29	7.06	5.04	3.76
2.92	2.23	81.26	47.90	30.26	20.37
10.02	2.23	45.85	29.01	19.14	13.45
20.69	2.23	24.41	16.54	11.50	8.56
30.31	2.23	13.37	9.42	6.86	5.35
2.92	3.31	132.02	74.79	45.59	29.67
9.94	3.31	70.57	42.43	27.41	19.26
19.90	3.31	33.35	21.19	14.52	10.68
29.83	3.31	14.53	10.18	7.47	5.76
2.92	4.97	321.54	177.93	102.65	64.38
10.11	4.97	126.10	76.32	48.39	31.67
19.90	4.97	46.82	30.10	20.15	14.53
29.79	4.97	16.54	11.60	8.58	6.64

From the data obtained from table 4.2, 3D curves were plotted with different concentrations of H_2O and CO_2 for the solution at constant temperature. Figure 4.13 shows the 3D plot for ChCl:MEA (1:6) solutions at 313.15 and 333.15 K. Rest of the curves could be found in Appendix B.3.1.

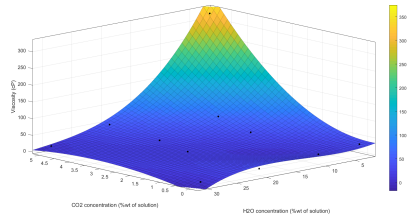

(a) Change in viscosity with different concentration of H_2O and CO_2 at 303.15 K for ChCl:MEA(1:6) solution

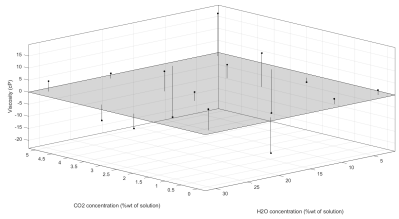

(b) Residual plot for viscosity curve of ChCl:MEA(1:6) solution with different concentrations of H_2O and CO_2 at 303.15 K

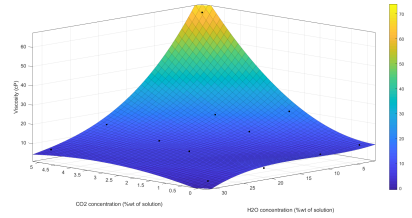

(c) Change in viscosity with different concentration of H_2O and CO_2 at 333.15 K for ChCl:MEA(1:6) solution

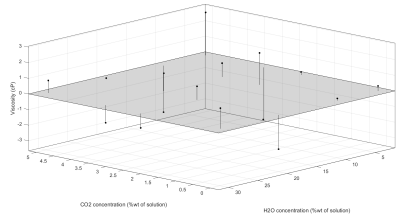

(d) Residual plot for viscosity curve of ChCl:MEA(1:6) solution with different concentrations of H_2O and CO_2 at 333.15 K

Figure 4.13: 3D curve for ChCl:MEA(1:6) solution comparing viscosity at different concentration of H_2O and CO_2 at 303.15 K and 333.15 K

Using a curve fitting tool the equation of the curves in the figure 4.13 is generated. Figure 4.13b and figure 4.13b represent the residual graph for the equation of the respected curve represented by the polynomial 4.2. As can be seen from the figures the residual plot shows a very small error in the actual and predicted values. In equation 4.2 $P_{00} - P_{31}$ are coefficients which vary with temperature, values for which are shown in table 4.3. Figure 4.14 shows the correlation for the predicted and experimental data for ChCl:MEA(1:6) solution predicted using equation 4.2. Based on the curve fir tool the average R^2 value for the equation 4.2 is 0.984 over all temperature ranges.

$$\mu(H_2O, CO_2) = P_{00} + P_{10}x + P_{01}y + P_{20}x^2 + P_{11}xy + P_{02}y^2 + P_{21}x^2y + P_{12}xy^2 + P_{03}y^3 \tag{4.2}$$

Where
x= CO_2 concentration in the solution [%wt of solution]
y= H_2O concentration in the solution [%wt of solution]

Table 4.3: Coefficients for the curve fit polynomial for ChCl:MEA(1:6) solution

Temperature (K)	P_{00}	P_{10}	P_{01}	P_{20}	P_{11}	P_{02}	P_{21}	P_{12}	P_{03}
303.15	41.97	7.068	-5.538	12.810	-3.138	0.471	-0.505	0.112	-0.0111
313.15	24.670	3.499	-2.603	7.015	-1.589	0.218	-0.275	0.057	-0.005
323.15	15.37	2.538	-1.273	3.852	-0.857	0.104	-0.150	0.0304	-0.003
333.15	10.42	2.021	-0.745	2.265	-0.508	0.060	-0.089	0.018	-0.001

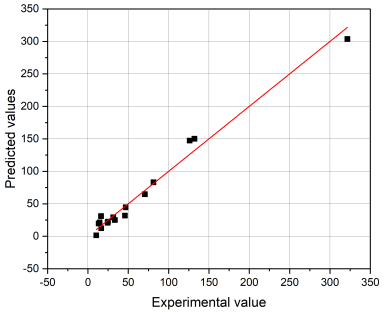

(a) correlation plot for predicted vs experimental values at 303.15K temperature

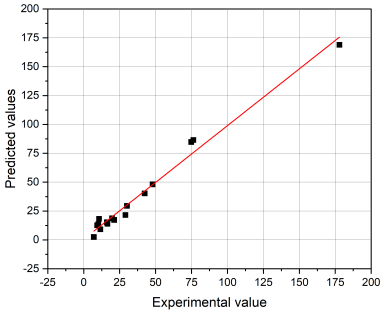

(b) correlation plot for predicted vs experimental values at 313.15K temperature

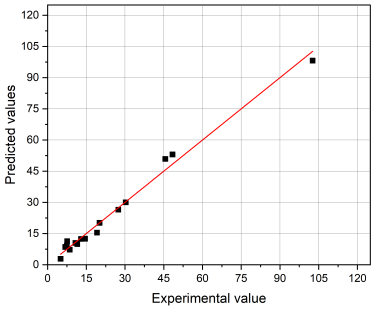

(c) correlation plot for predicted vs experimental values at 323.15K temperature

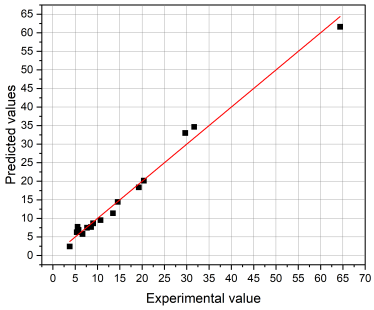

(d) correlation plot for predicted vs experimental values at 333.15K temperature

Figure 4.14: Correlation curves for predicted and experimental values at different temperature for ChCl:MEA(1:6) solution

Using the the equation 4.2, viscosites at different concentrations of H_2O and CO_2 were predicted at constant temperature. It was observed that at an given concentration the viscosity of the solvent follows the Arrhenius type equation over a temperature range. In order to determine the coefficients A_m and B_m for the equation 4.1, equation 4.2 was used to predict values for viscosity at different concentrations and different temperatures. A similar table to 4.2 was obtained which can be found in table B.2 Appendix B.3.1. From that table of predicted values the values for A_m

and B_m were calculated. The values for these coefficients are shown in table 4.4. The values obtained by this method are very close to the one obtained in the initial investigation, as shown in table 4.1. It is observed that as the CO_2 concentration in the solvent increases the activation energy represented by B_m also increases and addition of water reduces the activation energy. This increase in activation energy could be related to the formation of carbamates in the solution which are bigger molecules and as per the hole theory will find it difficult to mobilize. Addition of water as discussed before might cause an extension in the hydrogen bonds causing an increase in hole size hence, reducing viscosity and the activation energy of the solution.

Table 4.4: Coefficients for equation 4.1 ChCl:MEA(1:6) solution at different H_2O and CO_2 concentrations

Concentration		A_m (mPa.s)	B_m (K)	R^2
H_2O (%wt of solution)	CO_2 (%wt of solution)			
3.00	0.00	$4x10^{-5}$	-4100.6	0.999
9.95	0.00	$1x10^{-4}$	-3726.5	1
19.99	0.00	$5x10^{-6}$	-4709.3	0.998
2.92	2.23	$1x10^{-5}$	-4773	0.998
10.02	2.23	$4x10^{-4}$	-3450.4	0.999
20.69	2.23	$3x10^{-4}$	-3359.7	0.997
30.31	2.23	$6x10^{-5}$	-3860	0.998
2.92	3.31	$7x10^{-6}$	-5112.8	0.999
9.94	3.31	$5x10^{-5}$	-4250.6	0.999
19.90	3.31	$5x10^{-4}$	-3254.1	0.998
29.83	3.31	$7x10^{-5}$	-3812.2	0.997
2.92	4.97	$6x10^{-6}$	-5385.2	0.999
10.11	4.97	$1x10^{-5}$	-4884	0.999
19.90	4.97	$2x10^{-4}$	-3805.1	0.999
29.79	4.97	$2.9x10^{-4}$	-2527.3	0.998

Table 4.5 represents the Viscosity for ChCl:AMP(1:6) solution at different concentrations of H_2O and CO_2 and different temperature readings. As discussed before the AMP solution tends to form two phase solution when reacted with CO_2 and higher concentration of water needs to be added in order to remove the undissolved carbonates by reacting them with water as shown in reaction 2.3.

From the data obtained from table 4.5, a 3D curve was plotted. The 3D plots are plotted at different temperatures with different concentrations of H_2O and CO_2. Figure 4.15 shows the 3D plot for ChCl:AMP (1:6) solutions at 313.15 and 333.15 K. Rest of the curves could be found in Appendix B.3.1.

Table 4.5: Experimental values for viscosity of ChCl:AMP(1:6) solution with different concentration of H_2O and CO_2

Concentration		Viscosity (temperature) (cP)			
H_2O (wt% of solution)	CO_2 (wt% of solution)	303.15 K	313.15 K	323.15 K	333.15 K
10.07	0.00	115.60	63.60	35.46	22.11
20.07	0.00	51.19	30.50	19.26	13.39
30.02	0.00	26.61	16.69	11.13	8.06
40.05	0.00	13.95	9.07	6.43	4.66
10.00	0.77	108.46	58.69	32.83	19.89
19.99	0.77	56.59	33.50	20.92	14.17
30.23	0.77	25.89	16.10	10.64	7.59
39.99	0.77	13.68	8.88	6.14	4.42
30.66	1.16	28.27	17.58	11.62	8.06
40.08	1.16	13.84	8.95	6.10	4.38

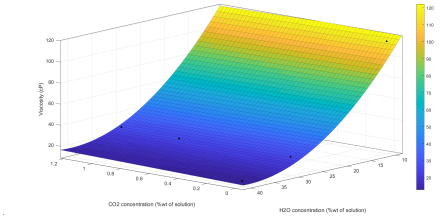

(a) Change in viscosity with different concentration of H_2O and CO_2 at 303.15 K for ChCl:AMP(1:6) solution

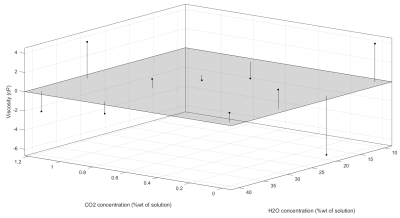

(b) Residual plot for viscosity curve of ChCl:AMP(1:6) solution with different concentrations of H_2O and CO_2 at 303.15 K

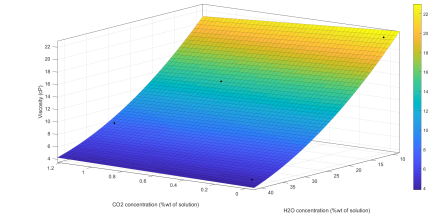

(c) Change in viscosity with different concentration of H_2O and CO_2 at 333.15 K for ChCl:AMP(1:6) solution

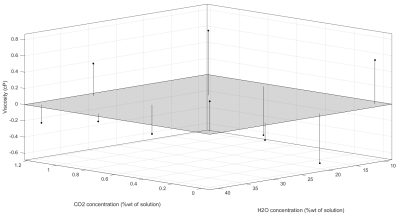

(d) Residual plot for viscosity curve of ChCl:AMP(1:6) solution with different concentrations of H_2O and CO_2 at 333.15 K

Figure 4.15: 3D curve for ChCl:AMP(1:6) solution comparing viscosity at different concentration of H_2O and CO_2 at 303.15 K and 333.15 K

Using a curve fitting tool the equation of the curves in the figure 4.15 is generated. Figure 4.15b and figure 4.15d represent the residual graph for the equation for the curve represented by the polynomial 4.3. As can be seen from the figures the residual plot shows a very small error in the actual and predicted values, and the error reduces at higher temperature indicating the equation to be more accurate at

higher temperatures. In equation 4.3 $P_{00} - P_{02}$ are coefficients which are dependent on temperature and values for which could be found in table 4.6. It is important to note that due to very low absorption of CO_2 and very high water concentration this equation is highly influenced by water concentration in the solution and hence, the polynomial is dependent on the square value of y and only linear in x.

$$\mu_{(H_2O,CO_2)} = P_{00} + P_{10}x + P_{01}y + P_{11}xy + P_{02}y^2 \tag{4.3}$$

Where
x= CO_2 concentration in the solution [%wt of solution]
y= H_2O concentration in the solution [%wt of solution]

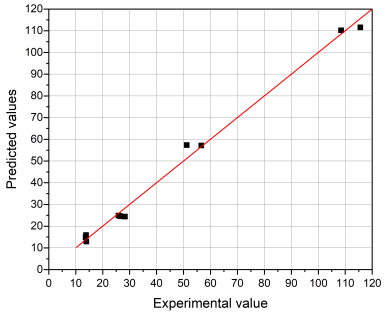

(a) correlation plot for predicted vs experimental values at 303.15 K temperature

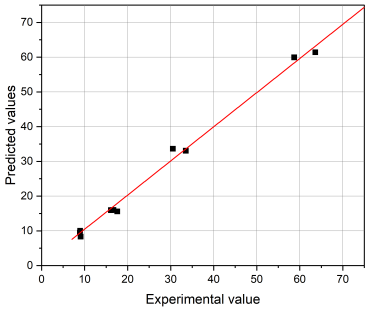

(b) correlation plot for predicted vs experimental values at 313.15 K temperature

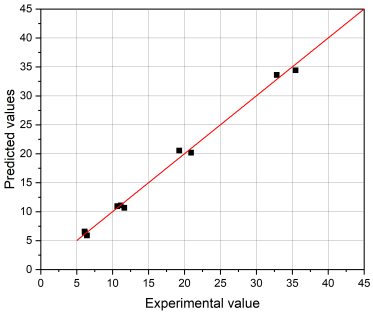

(c) correlation plot for predicted vs experimental values at 323.15 K temperature

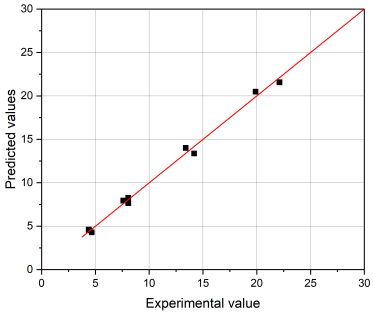

(d) correlation plot for predicted vs experimental values at 333.15 K temperature

Figure 4.16: Correlation curves for predicted and experimental values at different temperature for ChCl:AMP(1:6) solution

Figure 4.16 shows the correlation between the predicted value and the actual experimental value for ChCl:AMP(1:6) solution with different concentration of water and CO_2 calculated from the equation 4.3. Based on the curve fir tool used the

average R^2 value for the equation 4.3 is 0.993 over all temperature ranges.

Table 4.6: Coefficients for the curve fit polynomial for ChCl:AMP(1:6) solution

Temperature (K)	P_{00}	P_{10}	P_{01}	P_{11}	P_{02}
303.15	187.700	-3.970	-8.633	0.1631	0.1066
313.15	99.55	-3.421	-4.294	0.1222	0.05035
323.15	52.78	-1.773	-2.041	0.05866	0.02174
333.15	30.99	-2.047	-1.026	0.05801	0.00897

Using the the equation 4.3, viscosites at different concentrations of H_2O and CO_2 and at constant temperatures was predicted. It was observed that at an given concentration the viscosity of the solvent follows the Arrhenius type equation when compared with temperature. In order to determine the coefficients A_m and B_m for the equation 4.1, equation 4.3 was used to predict values for viscosity at different concentrations and different temperatures. A similar table to table 4.5 was obtained. Table B.3 in the Appendix B.3.1 gives the predicted values of viscosity, from the predicted values the values for A_m and B_m were calculated. The values for those coefficients are shown in table 4.7. The values obtained by this method are very close to the one obtained in the investigation of pure solvents, as shown in table 4.1. From the table 4.7 it can be seen that addition of water significantly reduces the activation energy which is represented by the absolute value of B_m, hence the viscosity reduces considerably. As discussed before this reduction might be because of the hydrogen bond stretching as discussed in section 4.2.1 .

Table 4.7: Coefficients for equation 4.1 for ChCl:AMP(1:6) solution at different H_2O and CO_2 concentrations

Concentration		A_m (mPa.s)	B_m (K)	R^2
H_2O (%wt of solution)	CO_2 (%wt of solution)			
10.07	0	$1x10^{-6}$	-5568.9	0.999
20.07	0	$8x10^{-6}$	-4774.3	0.998
30.02	0	$1x10^{-4}$	-3678.8	0.997
40.05	0	$6x10^{-5}$	-3700.3	0.997
9.998	0.77	$8x10^{-6}$	-5685.4	0.999
19.99	0.77	$5x10^{-6}$	-4904.1	0.999
30.23	0.77	$8x10^{-5}$	-3846.6	0.998
39.99	0.77	$2x10^{-5}$	-4027.9	0.999
30.66	1.16	$6x10^{-5}$	-3905	0.998
40.08	1.16	$2x10^{-5}$	-4193.1	0.999

4.4.2. Electrical conductivity

Electrical conductivity of the solvent is important parameter for selecting the most suitable solvent for the process as higher electrical conductivity will result in lower

Ohmic losses. In the previous section the effect of water and CO_2 on the electrical conductivity was discussed. It was established that electrical conductivity is highly dependent on the viscosity of the solution and as the viscosity decreases the conductivity increases. This section discusses the effect different concentrations of CO_2 and water have on the conductivity of the solution. A polynomial equation is derived to predict the electrical conductivity of the system at different concentrations of water and CO_2.

Table 4.8: Experimental values for electricacl conductivity for ChCl:MEA(1:6) solution with different concentrations of H_2O and CO_2

Concentration		Electrical Conductivity (mS/cm)
H_2O (%wt of solution)	CO_2 (%wt of solution)	
3.00	0.00	2.89
10.00	0.00	3.75
20.00	0.00	5.53
30.00	0.00	8.17
2.92	2.23	2.16
10.02	2.23	3.32
20.69	2.23	5.98
30.31	2.23	9.69
2.92	3.31	1.66
9.94	3.31	2.89
19.90	3.31	5.67
29.83	3.31	10.32
2.92	4.97	0.92
10.11	4.97	2.09
19.90	4.97	5.25
29.79	4.97	10.87

Table 4.8 shows the experimental value for electrical conductivity in ChCl:MEA(1:6) solution at different concentrations of H_2O and CO_2. From the above data a 3D curve was plotted as shown in figure 4.17a. From the 3D plot a polynomial fit was generated using curve fitting tool, this polynomial is represented by equation 4.4. As discussed earlier the conductivity of the solution was measured at one temperature because in the lab maintaining higher temperatures is not possible.

$$\sigma_{(H_2O,CO_2)} = 3.24 - 0.412x - 0.046y - 0.042x^2 + 0.036xy + 0.007y^2 \quad (4.4)$$

Where
x= CO_2 concentration in the solution [%wt of solution]
y= H_2O concentration in the solution [%wt of solution]

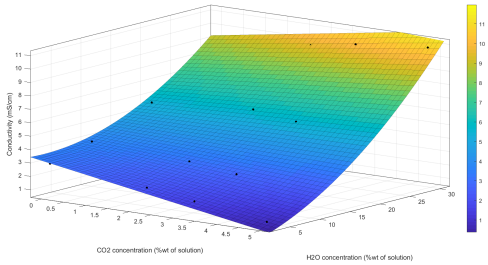

(a) Change in electrical conductivity with different concentration of H_2O and CO_2 at 294.15 K for ChCl:MEA(1:6) solution

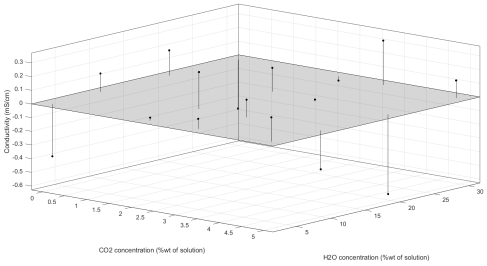

(b) Residual plot for electrical conductivity plot of ChCl:MEA(1:6) solution

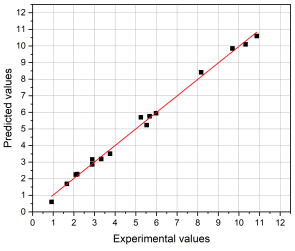

(c) correlation plot for predicted vs experimental values at 294.15 K temperature

Figure 4.17: 3D curve for ChCl:MEA(1:6) solution comparing electrical conductivity at different concentration of H_2O and CO_2 at 294.15K with residual curve and correlation curve

From figure 4.17a it can be observed that as the CO_2 concentration increases the electrical conductivity decreases. This is in correlation to increasing viscosity as discussed before, the viscosity has a big effect on electrical conductivity. Increasing water concentration in the solution also increases the conductivity. At a concentration of 30% water the electrical conductivity is around 10 mS/cm which is closer to the target value to 11 mS/cm as discussed in section 2.4.5. From equation 4.4 it is evident that water has a higher effect on conductivity as increasing water concentration increases conductivity more than the reduction observed with increasing CO_2 concentration. From table 4.8 it can be seen that conductivity for the solution is similar at similar water concentrations.

Figure 4.17b gives the residual plot obtained from comparing the predicted to actual value for conductivity for ChCl:MEA(1:6) solution using the equation 4.4. From the figure it is evident that the error is very small and the curve fit tool gives an R^2 value of 0.998 to the equation 4.4. Figure 4.17c shows the correlation between the predicted and the experimental value obtained from equation 4.4, it can be seen that the equation has high correlation with the predicted values.

Table 4.9: Experimental values for electricacl conductivity for ChCl:AMP(1:6) solution with different concentrations of H_2O and CO_2

Concentration		Electrical Conductivity (mS/cm)
H_2O (%wt of solution)	CO_2 (%wt of solution)	
10.00	0.00	0.49
20.07	0.00	1.27
30.02	0.00	2.64
40.05	0.00	4.55
10.00	0.77	0.45
19.99	0.77	1.23
30.23	0.77	2.64
39.99	0.77	4.80
25.06	1.16	1.85
30.66	1.16	2.58
35.00	1.16	4.08
40.08	1.16	4.71
10.00	1.55	0.00
30.10	1.55	2.61
35.05	1.55	3.72
40.08	1.55	4.74

Table 4.9 shows the electrical conductivity of ChCl:AMP (1:6) solution with different concentrations of H_2O and CO_2 at 294.15 K. From the above data a 3D curve was plotted as shown in figure 4.18. From the plot a polynomial fit was generated using curve fitting tool, this polynomial is represented by equation 4.5.

$$\sigma_{(H_2O,CO_2)} = 30.377 - 0.4566x - 0.01308y + 0.01553xy + 0.002958y^2 \quad (4.5)$$

Where
x= CO_2 concentration in the solution [%wt of solution]
y= H_2O concentration in the solution [%wt of solution]

From figure 4.18a it can be observed that as the CO_2 concentration increases the electrical conductivity decreases. Increasing water concentration in the solution also increases the conductivity. At H_2O concentration of 40%wt of solution, the electrical conductivity is around 4 mS/cm which is very far from to the target value to 11 mS/cm. From equation 4.5 it is evident that water has a higher effect on conductivity. Electrical conductivity of ChCl:AMP(1:6) is less when compared with all the selected solvents, along with the property of AMP to form AMP-carbamates which are unstable and precipitate it is not the solution suitable for the process.

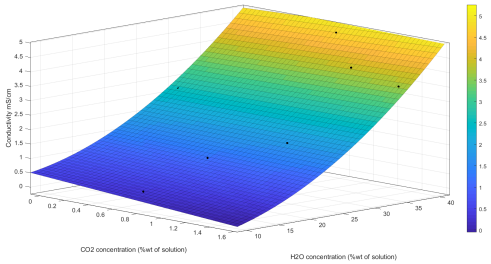

(a) Change in electrical conductivity with different concentration of H_2O and CO_2 at 294.15 K for ChCl:AMP(1:6) solution

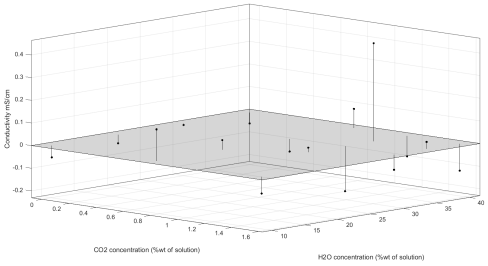

(b) Residual plot for electrical conductivity plot of ChCl:AMP(1:6) solution

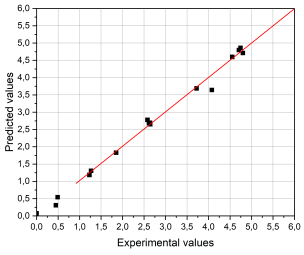

(c) correlation plot for predicted vs experimental values at 294.15K temperature

Figure 4.18: 3D curve for ChCl:AMP(1:6) solution comparing electrical conductivity at different concentration of H_2O and CO_2 at 294.15K with residual curve and correlation curve

4.5. Effect of adding organic solvent

Until now in this thesis study the physico-chemical properties of the the solutions have been determined. It is established that adding CO_2 in amine based solvent increases viscosity and reduces conductivity and adding water has the opposite effect. The effect of $CO_2$is however very less on ChCl:EG solutions since CO_2 is only physically absorbed instead of chemical absorption. Adding water in amine solution increases the conductivity of the solution to about 10 mS/cm when the water concentration is about 30 %wt of the solution but as discussed in section 2.4.5 having higher water concentration in the solution is not desirable for the electrochemical conversion process.

As discussed in the section 2.3.3 the limiting factor for CO_2 apart from the chemical kinetics is higher viscosity as it hinders diffusion. The limiting factor for electrochemical conversion process is lower conductivity, which is also dependent on viscosity. It is important to find an alternate to adding water in the solution to reduce viscosity and increase conductivity. In this section, the effect of adding MEA and AMP is noted on the ChCl:EG. MEA/AMP solutions are added to ChCl:EG solution instead of the other way round since amines have shown higher potential of CO_2 absorption compared to ChCl:EG solution as shown previously. Also varying

the quantity of amines in the solution will help understand the effects of diffusion and how viscosity limits CO_2 absorption. The solutions are prepared by the method described in the section 3.1.1.

4.5.1. CO_2 absorption

The physics of CO_2 absorption is described in section 2.3.3, it is known that CO_2 absorption in the bulk of the solution is limited by viscosity as the increase in viscosity due to formation of carbamates limit the absorption of the gas in the bulk of the system. In this section all the solvents prepared with adding AMP and MEA in ChCl:EG solutions are loaded with CO_2 using the CO_2 loading set up described in section 3.3 for exactly 30 minutes. This time limit is set based on the loading capacity. It was determined that at the flow rate ChCl:EG:MEA(1:2:9) solution almost reached the maximum loading capacity, In order to compare the solutions the CO_2 absorbed in the solution was kept constant varying the concentration of the solution and measuring the effect it has on viscosity and electrical conductivity. The amount of CO_2 was measure using barium chloride test.

All the solutions contain AMP formed a 2 phase solution. Different configurations of the solutions were tried but a two phase solution was obtained unless higher concentration of water was added. This method is attempting to remove water from the solution hence, AMP solutions were removed from the test and only solutions containing MEA were tested.

Table 4.10: CO_2 absorption for different concentrations of MEA in different ChCl:EG solutions

Base solvent	Moles of MEA (moles/l)	CO_2 (wt% of solution)	CO_2 (mol CO_2/mol MEA)
ChCl:EG (1:2)	3.10	3.95	0.34
	6.17	4.97	0.22
	9.20	6.04	0.17
ChCl:EG (1:3)	3.06	3.75	0.32
	6.15	4.83	0.21
	9.19	6.44	0.18
ChCl:EG (1:4)	3.07	3.56	0.32
	6.13	5.43	0.24
	9.18	6.33	0.19

Figure 4.19 graphically shows the amount of CO_2 absorbed in different ChCl:EG solutions as observed from table 4.10. It is interesting to observe that the CO_2 concentration in terms of mol CO_2/mol MEA decreases as the concentration of MEA increases. On the contrary the amount of CO_2 absorbed in the system (%wt of solution) increases as the moles of MEA increases. The unit mol CO_2/mol MEA is a measure of how easy is for CO_2 molecules to reach the MEA atom. A higher mol CO_2/mol MEA value indicates a higher diffusion of the gas in the liquid phase. In theory all molecules of MEA can react with CO_2 but the kinetics and equilibrium of the reactions dictates that the maximum is around 0.5 mol CO_2/mol MEA. The

closer the solution is to this maximum the better is the solution for CO_2 absorption.

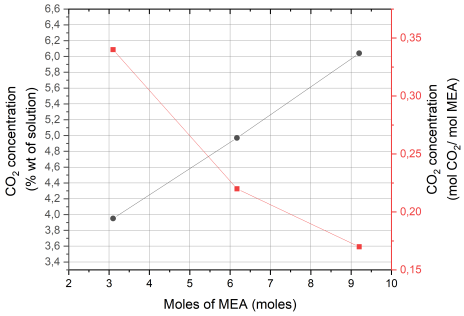

(a) Concentrations of CO_2 absorbed in the ChCl:EG (1:2) solution with different concentration of MEA

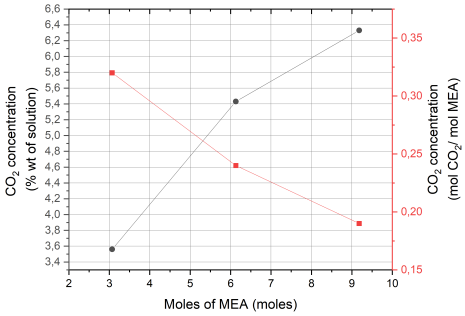

(b) Concentrations of CO_2 absorpbed in the ChCl:EG (1:4) solution with different concentration of MEA

Figure 4.19: CO_2 absorption in different ChCl:EG solutions for different concentrations of MEA in the solution

Figure 4.20 Shows the FTIR spectrum for CO_2 rich solution of ChCl:EG. It is important to note that the peaks observed due to formation of carbamates due to reaction of CO_2 with MEA are at wavenumber 1307 cm^{-1} which is same as the one observed for ChCl:MEA solutions as depicted by figure 4.11. It can be clearly seen that higher amounts of MEA in the solution results in higher absorbance value, as mentioned before the CO_2 loading is not at equilibrium loading capacity. Figure B.8 in Appendix B.4.1 compares the CO_2 absorption for ChCl:EG(1:4) solution with 3 moles of MEA, with CO_2 purged for 60 minutes and 30 minutes.

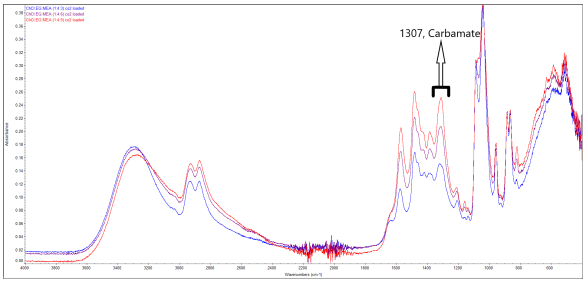

(a) FTIR spectrum for CO_2 rich solvent for different concentration of MEA

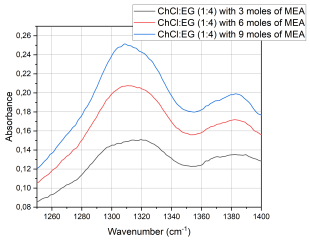

(b) Zoomed in FTIR spectrum for CO_2 rich solvent for different concentration of MEA

Figure 4.20: FTIR spectrum for CO_2 rich ChC:EG solution with different concentration of MEA

4.5.2. Viscosity

From figure 4.21a it can be seen that ChCl:EG(1:2) solution has a higher viscosity than ChCl:EG(1:3) and ChCl:EG(1:4) solutions. From figure 4.21b it can be

seen that a solution of ChCl:EG(1:2) with CO_2 concentration of 6.04 %wt of solution has viscosity of about 317.7 cP which is comparable to viscosity observed in ChCl:MEA (1:6) solution with CO_2 concentration of 4.97 %wt of solution with same concentration of water (3%wt of solution) as obtained from table 4.2.

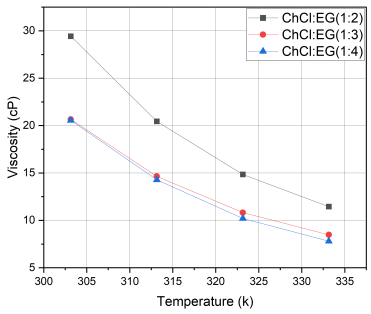

(a) Viscosity comparison for pure ChCl:EG solutions

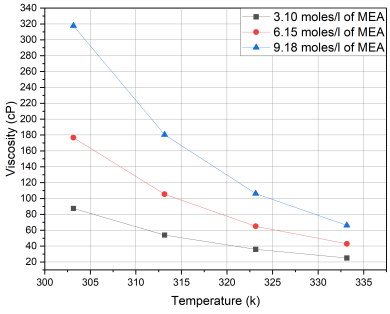

(b) Change in viscosity for CO_2 rich ChCl:EG(1:2) solutions at different concentration of MEA

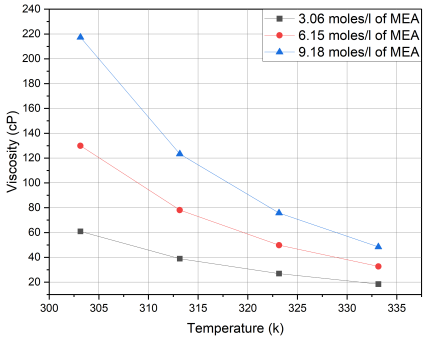

(c) Variation of viscosity with temperature for CO_2 rich ChCl:EG(1:3) solutions with different concentration of MEA

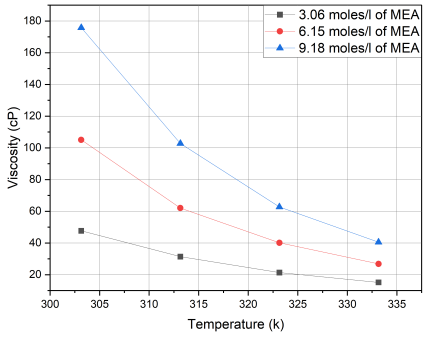

(d) Variation of viscosity with temperature for CO_2 rich ChCl:EG(1:4) solutions with different concentration of MEA

Figure 4.21: Viscosity comparison for pure and CO_2 rich ChCl:EG DES with different concentration of MEA

Figure 4.21c and 4.21d shows the viscosity for ChC:EG(1:3) and ChC:EG(1:4) solution with different concentration of MEA, from the figure it is observed that increasing concentration f MEA increases the viscosity for CO_2 rich solvents. When the concentration of MEA is low in the solution the concentration of CO_2 (%wt of solution) absorbed in the solution is low hence the concentration of carbamates in the solution are lower. From section 2.4.4 it was inferred that the viscosity of the solution is dependent on the probability of a molecule finding a void/hole to move through, since the concentration of carbamates is lower the probability of the molecules to find a void/hole is higher hence at lower concentrations of MEA the viscosity of the solution is lower. This is beneficial because as discussed in the

previous section reducing viscosity increases diffusion in the solution. Diffusion is a limiting factor for CO_2 absorption and reducing viscosity will increase diffusion in the system.

In the section 4.5.1, it was discussed that the unit mol CO_2 / mol MEA is an important parameter to understand the diffusion in the bulk of the solution. In figure 4.22b it is evident that as the moles of MEA increases the viscosity of the viscosity increases and the mol CO_2 / mol MEA in the solution decreases. Comparing figure 4.21d and figure 4.19b the concentration of CO_2 in terms of %wt of solution increases with increases in moles of MEA along with the viscosity of the solution but the mol $CO2$/ mol MEA decreases indicating that the gas is not able to reach the bulk of the solution and hence a lot of MEA molecules in the solution remain unreacted. Diffusion is a limiting factor for CO_2 absorption and if the viscosity of the solutions reduces more gas can be diffused in the solution.

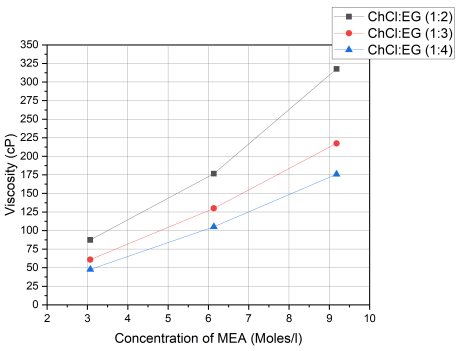

(a) Variation of viscosity with concentration of MEA for CO_2 rich ChCl:EG solutions at 303.15 K

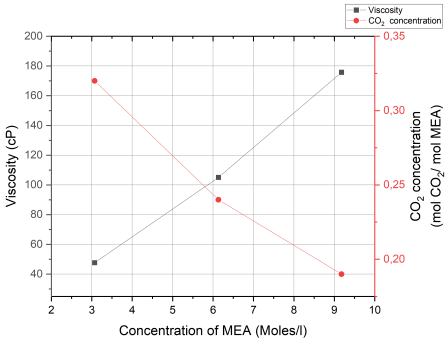

(b) Comparing change in viscosity with moles of MEA in ChCl:EG:MEA(1:4:3) solution

Figure 4.22: Viscosity comparison CO_2 rich ChCl:EG DES with different concentration of MEA and CO_2

4.5.3. Electrical conductivity

To prevent Ohmic losses in the solvent it is important for the solvent to have good electrical conductivity. In the previous section it was discussed that as the CO_2 concentration in ChCl:MEA/AMP solution increases the electrical conductivity decreases. As established before the electrical conductivity is inversely dependent on the viscosity of the solution. From figure 4.2 it can be seen that ChCl:EG has the highest conductivity among the selected DES.

From figure 4.23a it can be observed that adding MEA in the ChCl:EG solution reduces the conductivity. This happens because addition of MEA increases the viscosity of the solution. From figure 4.23c it can be seen as the moles of MEA increases the viscosity of the solution increases and the conductivity decreases. Among the pure solution ChCl:EG (1:4) has the highest conductivity followed closely by ChCl:EG(1:3) and the viscosities of the two solution are very close as shown in figure 4.21a. Figure 4.23b shows the change in conductivity for a CO_2 rich solution. The amount of CO_2 absorbed is same as discussed in section 4.19. It can be clearly

seen as the concentration of mea increases the concentration of absorbed CO_2 (%wt of solution) increases and the viscosity increases hence, the conductivity decreases. Figure 4.23d shows the change in conductivity for a CO_2 rich solvent at different concentration of MEA.

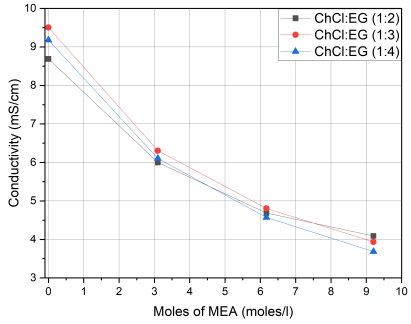

(a) Conductivity compared with different concentrations of MEA for pure ChCl:EG solutions

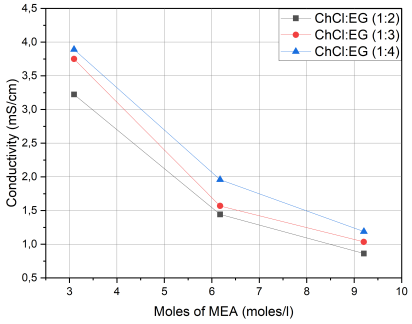

(b) conductivity compared with different concentrations of MEA for CO_2 rich ChCl:EG

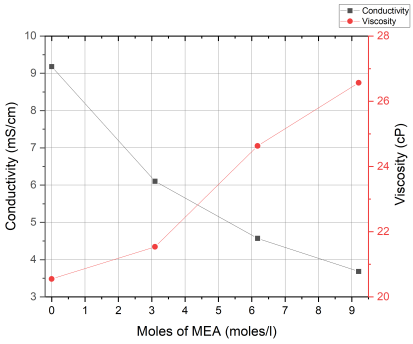

(c) Comparing conductivity and viscosity of pure ChCl:EG (1:4) solution with different concentration of MEA

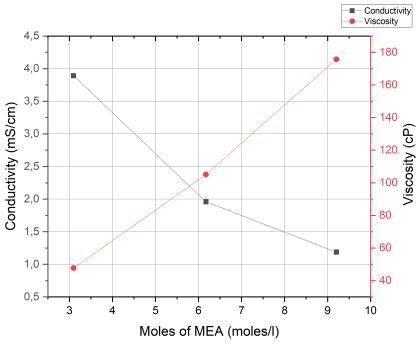

(d) Comparing conductivity and viscosity of CO_2 rich ChCl:EG (1:4) solution with different concentration of MEA

Figure 4.23: Comparing changes in conductivity of solution with different concentration of MEA and effect of CO_2 absorption

5

Conclusions and Recommendations

5.1. Conclusion

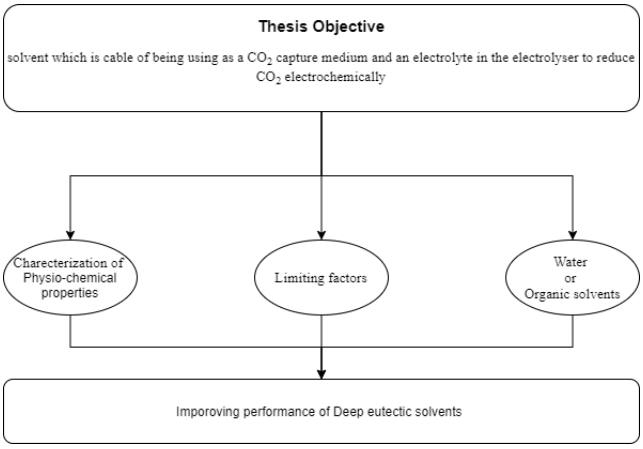

Figure 5.1: Research objective

The main objective of this thesis is to find a solvent that is a good medium for CO_2 capture and an electrolyte for electrochemical conversion of CO_2 process. DES are a form of IL which have gained a lot of attention in recent years due to their desirable properties such as biodegradability, low vapor pressure, and high tunability for the required purpose. Research has shown promising results in the application of DES on the field of CO_2 capture at a lower price with more eco-friendly solvent. Choline chloride is the most widely used quaternary amine salt which has all the desirable properties, when combined with a CO_2 philic hydrogen bond donor group such as

amines groups this solvent has potential for being used for CO_2 capture. It is hence was important to determine the Physico-chemical properties of these solvents.

5.1.1. physico-chemical properties

Viscosity

- The viscosity for DES is a factor of temperature, as the temperature increases the viscosity decreases. Viscosity follows Arrhenius equation, represented by equation 2.10 showing an exponential relation with temperature.

- The viscosity of the solution is dependent on the probability of the molecules in the solution to find a void/hole and not the thermodynamics of formation of void/hole as discussed in the Hole theory in section 2.4.4. At any given time, the fluid will have a distribution of cavity sizes, and the ions/molecules will only be able to move if the adjacent cavity of a suitable dimension is available. Hence, it is assumed that only a few ions/molecules will be able to move at any given moment of time, giving rise to higher viscosity. At higher temperatures, the hole size increases as the surface tension decrease as per the equation 2.13 hence, reducing viscosity.

- Viscosity of solution can be visualised with the activation energy (E_μ), the larger the molecule, higher the activation energy. Larger molecules will have difficulty moving through the voids therefore, they higher activation energy. AMP has the largest molecular size among the selected DES and hence the largest activation energy. ChCl:AMP(1:6) has viscosity of 115.6 mPa.s which is the highest among the selected solvents followed by ChCl:MEA(1:5) and ChCl:MEA(1:6) at 35.1 mPa.s, and 31 mPa.s respectively.

- Addition of water in the solution reduces viscosity. This contradicts the explanation given by hole theory which states that the addition of a liquid of lower surface tensions will reduce viscosity. Addition of water can increase the hole size by stretching the hydrogen bonds in the presence of oxygen molecules. This could be visualised from the figure 4.6b, in the presence of water, the oxygen molecule tends to pull the hydrogen molecule causing the bond to stretch hence reducing the viscosity.

- Amine based solvents react with CO_2 to form carbamates or bicarbonates as shown in reactions 2.2 and 2.3 respectively. The product formation depends on the amine used, primary amines form carbamates upon reacting with CO_2 whereas tertiary amines form bicarbonate in the presence of water. AMP is a sterically hindered primary amine which forms unstable carbamates which on reaction with water forms bicarbonates. In absence of water, AMP-carbamates are formed which precipitates and is only soluble in water.

- The effect of formation of carbamates is seen in the viscosity of the solution as increasing the amount of CO_2 absorbed in the solution increases the viscosity significantly. This increase in viscosity is however a limiting factor for absorp-

tion of CO_2 as increase in viscosity of the solution reduces the diffusion in the bulk of the liquid.

Electrical conductivity

- Higher conductivity is desired for reducing ohmic losses in the electrochemcial reduction process. Electrical conductivity is dependent on the viscosity of the solution. Higher viscosity in the solution will hinder the ion mobility through the solution.
- ChCl:EG(1:3) DES has the highest conductivity of 9.51 mS/cm.
- Among the amine based DES, ChCl:AMP has the highest viscosity and the least conductivity of 0.49 mS/cm.
- Addition of water in the solution reduces viscosity significantly and hence increases conductivity. A reduction in viscosity increases the ion mobility of the solution. The effect of the addition of water can be seen most distinctly for ChC:AMP solution whose electrical conductivity increases from 0.48 mS/cm to 4.55 mS/cm when water concentration rose from 10% to 40% wt of solution.
- Absorption of CO_2 in the amine based DES increases the viscosity and hence reduces the conductivity of the solution. The change in viscosity is exponential when compared to the concentration of CO_2, when concentration of CO_2 in ChCl:MEA(1:6) solution changes from 0% to 8.4% wt of solution, the viscosity increases from 32.35 to 2629.3 cP and the conductivity cannot be measure because of such high viscosity.
- Higher water content is not desired for the electrochemical conversion process. At lower water content, hydrogen evolution reaction suppresses and it causes to improve the CO_2 reduction reaction.

5.1.2. Limiting factor

In the next stage, it is important to know the limiting factors for the solution. In section 2.3.3, it was discussed that absorption of CO_2 is limited by the diffusion of the gas in the bulk solution. Reducing the viscosity is crucial to increase the diffusion in solution.

- CO_2 absorption process is limited by viscosity of the solution, higher viscosity hinders the diffusion of the gas in the bulk of the solution.
- Viscosity of the solution increases significantly with absorption of CO_2, at a concentration of concentration of 8.4 %wt of solution has viscosity 2629.03 mPa.s at 303.15 K. It was observed that no more CO_2 could be loaded even though the mol/mol concentration of CO_2 about 1.63 mol CO_2 / mol MEA. As discussed before a lower mol/mol value for CO_2 absorption indicates that the gas is not able to reach sufficient molecules in the solution hence the diffusion is reduced because of high viscosity.

- It was found that increasing temperature reduces viscosity, but since the carbamate formation reaction is an exothermic reaction, increasing the temperature will not favour the reaction.

5.1.3. Addition of organic solvent

Adding organic solvent instead of water can also reduce viscosity and increased conductivity as discussed in section 2.4.5. Hence, different concentrations of MEA and AMP were added to ChCl:EG DES to determine its effect on viscosity and electrical conductivity and CO_2 absorption.

- ChCl:EG solution performs physical absorption of CO_2 unlike chemical absorption in amine based DES. The amount of CO_2 dissolved is very less as the pressure is less compared to the high pressures required for physical absorption.
- Addition of MEA and AMP in ChCl:EG solutions increases the CO_2 absorption significantly.
- Reducing the concentration of EG in the ChCl:EG:MEA solution increases the viscosity and reduces electrical conductivity.
- Increasing the concentration of EG in the solution reduces viscosity and increases electrical conductivity for the same concentration of MEA. This is because EG has a lower surface tension so addition of a fluid with lower surface tension reduces viscosity as per the equation 2.13. MEA has a surface tension higher than EG hence addition of MEA increases viscosity and reduces electrical conductivity.
- Increasing the concentration of MEA in the solution increases the amount of CO_2 absorbed in the solution hence the concentration of CO_2 in %wt of solution increases but the concentration of CO_2 in terms of moles of CO_2/ moles of MEA reduces. This is due to the fact that the viscosity increases with increase in the concentration of carbamates formed from the reaction of MEA and CO_2 this increase in viscosity reduces the diffusion in the solution hence hindering more MEA to react with CO_2. Viscosity of the solution is dependent on the probability of the molecules to find suitable void/hole to fit through and with lower concentrations of MEA a lower concentration of carbamates are formed increasing the probability of molecules to pass through the voids/holes hence, reducing viscosity.
- Absorption of CO_2 also reduces electrical conductivity but the drop in conductivity is not as significant as observed for ChCl:MEA solutions.

Addition of EG in the DES significantly improves the performance of the DES. Based on the experiments conducted and the results obtained, it is concluded that ChCl:EG:MEA (1:4:3) is the ideal solution for the process. A CO_2 rich solution of ChCl:MEA(1:6) at CO_2 loading of 3.5 %wt of solution, has the viscosity 132.02 cP

and the electrical conductivity of 1.66 mS/cm. At similar loading, the viscosity of ChCl:EG:MEA (1:4:3) is 47.68 cP which is almost 63.88% less and the electrical conductivity is 3.892 mS/cm which is 134.45 % more than ChCl:MEA(1:6).

5.2. Recommendation For future studies

The following are some recommendations for future experiment:

1. Changing the CO_2 concentration in ChCl:EG:MEA solutioin
    - Properties such as surface tension, viscosity and conductivity at different concentrations of CO_2 should be characterised and the dependency to temperature should be quantified.
2. Vapour Liquid Equilibrium (VLE) test
    - Getting VLE data for different temperatures could be used to calculate the heat of absorption for the solution. It will be interesting to observe how the heat of absorption changes in the presence of QAS like ChCl.
    - From the results it was observed that diffusion gas for ChCl:EG:MEA (1:4:3) solution is high, VLE test at lower pressure could show interesting results.
3. Using different CO_2 loading setup
    - A lower mass flow rate for CO_2 could be used in order to determine the kinetics of the reactions.
    - A different CO_2 loading setup could be used with mixing gases such as N_2 and O_2 so see the effect of them on the solution.
    - A lower concentration of CO_2 mixture could be obtained by adding a separate channel with higher mass flow rate of another gas so as to compare the CO_2 absorption properties at lower partial pressures.

A

Additional Sample preparation

A.1. Pure sample preparation

To make pure deep eutectic solution the following procedure

1. The ceramic bowl and glass bottles are rinsed and washed carefully. They are dried in the oven for 10-15 minutes until fully dry

2. Transfer the required amount of choline chloride into the ceramic bowl shown in figure A.1a. Place the bowl in the oven shown in figure A.1b at 110 ^{o}C for 2 hr.

3. Transfer the choline chloride into a glass bottle. Add the HBD in the same bottle according to the molar ratio.

4. Put the glass bottle on the magnetic stirrer as shown in figure A.1c and set the temperature according to the solution as mentioned in figure 3.1.

5. After about 1-2 hrs add water according to solution as mentioned in figure 3.1 and then Still until a clear solution is observed as shown in figure A.1d

6. The resulting solution will result in clear solution with 3% wt water solution and 97% pure DES.

A

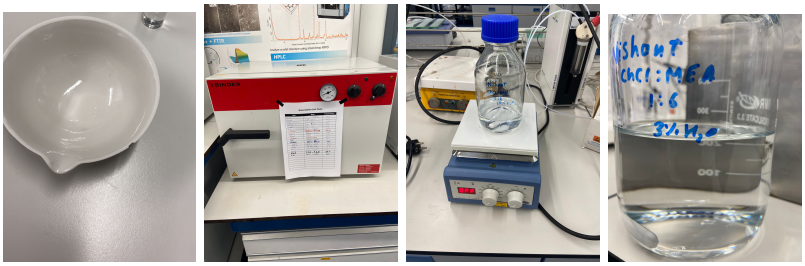

(a) Ceramic bowl (b) Oven (c) Magnetic Stirrer (d) Clear solution

Figure A.1: Instruments for sample preparation

A.2. Organic solvent mixing tables

Base Solution	MEA (g)	Volume of ChCl:EG (ml)	Moles of MEA (mol)	Molarity (mol/L)
ChCl:EG (1:2)	13.09	69.22	0.21	3.10
	23.34	61.89	0.38	6.17
	30.63	54.48	0.50	9.20
ChCl:EG (1:3)	12.94	69.27	0.21	3.06
	23.09	61.47	0.38	6.15
	30.69	54.68	0.50	9.19
ChCl:EG (1:4)	14.12	75.29	0.23	3.07
	26.10	69.65	0.43	6.13
	34.71	61.91	0.57	9.18

Table A.1: Prepared samples of different molarities of MEA in ChCl:EG solution

Solution	AMP (g)	Volume of ChCl:EG (ml)	Moles of AMP (mol)	Molarity (mol/L)
ChCl:EG (1:3)	22.41	75.28	0.23	3.01
	33.86	56.89	0.34	6.01
	42.26	47.34	0.43	9.01
ChCl:EG (1:2)	20.01	67.30	0.20	3.00
	32.94	55.50	0.33	5.99
	43.33	48.60	0.44	9.00

Table A.2: Prepared samples of different molarities of AMP in ChCl:EG solution

A.2.1. AMP CO_2 Dillution tables

Co_2 Loaded sample (g)	Pure sample (g)	Co_2 in the sample (wt% of solution)
59.98	240.67	0.77
86.34	201.81	1.16
120.07	180.18	1.55
300	0.00	3.88

Table A.3: CO_2 Dilution with adding pure sample to CO_2 loaded ChCL:AMP (1:6) Sample

CO_2 Concentration (%wt of solution)	weight of sample (gm)	water added (gm)	Water Concentraion (%wt of solution)
0.774	87.000	0.000	10.012
	77.280	9.653	19.994
	70.706	20.495	30.225
	59.496	29.740	39.995
1.163	80.870	16.253	25.061
	70.397	20.970	30.656
	72.558	27.900	34.996
	62.141	31.191	40.077
1.552	93.360	0.000	10.012
	63.631	18.302	30.104
	76.871	29.652	35.053
	63.485	31.875	40.083
0	73.662	9.285	20.075
	63.047	18.040	30.023
	64.867	32.522	40.055

Table A.4: CO_2 loaded ChCl:AMP (1:6) Sample Dilution with adding H_2O

B

Additional measurements

B.1. Density

B.1.1. Density of pure solvents

Figure B.1 shows the density for different DES over a temperature range from 293.15-333.15 K. The density of DES changes linearly with respect to temperature as given by the equation B.1 as discussed in section 2.4.2. Table B.1 compares parameters a and b from the equation 2.9 for experimental data to the data available in literature. We can observe that the values obtained experimentally are very similar to the available literature. No literature was available for ChCl:EG (1:3) and ChCl:AMP (1:6) solution. It is also important that the R^2 value for these experiments was quite high. From figure we can observe that ChCL:AMP (1:6) is the least dense solution, one reason can be because of higher water concentration (10% wt) which reduces Density. ChCl:EG (1:2) has the highest density of about 1.1195 g/cm^3, among the MEA DES ChCL:MEA(1:5) have lower density of about 1.05141.

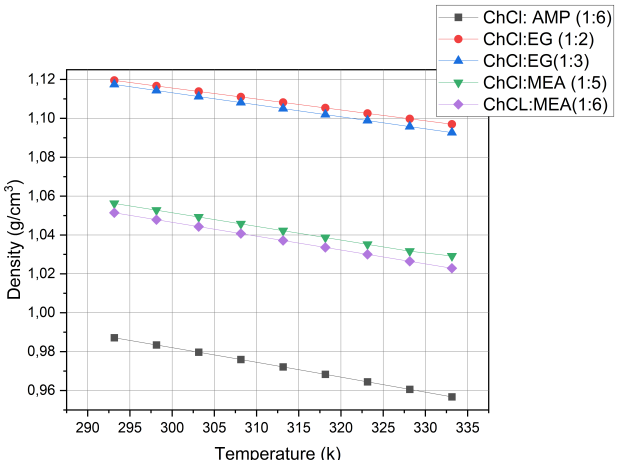

Figure B.1: Density comparison of different DES over a range of temperature

$$\rho = a + bT \tag{B.1}$$

Table B.1: Comparing Experimental parameters and regression coefficients to values obtained from literature for density parameters for different DES

Solvent	a (g/cm^3)		b (g/cm^3.k)		R^2
	Experimental	Literature	Experimental	Literature	
ChCl:EG (1:2)	1.1307	1.13	-0.0006	-0.0006	1
ChCl:EG (1:3)	1.1303	-	-0.0006	-	0.999
ChCl:MEA (1:5)	1.258	1.283	-0.0007	0.0006	0.999
ChCl:MEA (1:6)	1.26	1.286	-0.0007	0.0007	1
ChCl:AMP (1:6)	1.210	-	-0.0008	-	0.999

B.1.2. Effect of water on Density

Figure B.2 shows the variation in Density with different water concentrations in the solution. From figure B.2a it can be seen the density does not change significantly at a specific temperature, the change in density is about 0.014 g/cm^3 at 298.15K when the concentration of water changes from 3% to 20%. Also The change with temperature is is similar to what was observed in pure solvents as expressed by equation B.1. It can be observed from figure B.2b that the density goes from 1.117 to 1.103 gm/cm^3 at constant temperature of 293.15 K. Similar effects was observed for different solvents as well.

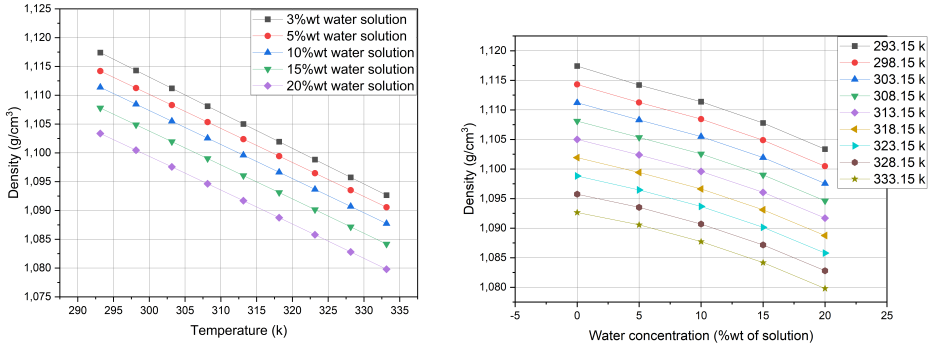

(a) Density vs Temperature curve with varied water concentration

(b) Isothermal comparison of density with varied water concentration

Figure B.2: Effect of adding water on density of ChCl:EG (1:3) solution

B.2. CO_2 absorption in AMP

Figure B.4 shows the FTIR plot forAMP with different concentrations of water. Three different solvents were tested with water concentrations of 10%, 15% and 20%. These solvents were Loaded with CO_2 for different amount of time, it was observed that solution with 10% water formed the precipitate the fastest and higher water concentrations could absorb higher amount of CO_2. Different solvents were also tested such as DMSO and Propaline carbonate but a precipitate was alwas foemed at lower concentrations of water. The precipitate would only desolve at higher concentrations of water.

Figure B.3 shows the CO_2 loaded samples with different concentration of CO_2, CO_2 was loaded for 33 min and 45 minutes and a two phase solution was observed in all the solutions.

Figure B.5 shows the FTIR spectrum for ChCl:AMP (1:6) with 10%wt water represented in blue, 20%wt water represented in purple and 10%wt DMSO and 10%wt water solution. From the spectrum it can be seen that both 20%wt water solution and 10%wt DMSO with 10% water solutions have similar curve at the same loading time, the peaks are identical indicating that addition of organic solvent did not have any effect on the solution

Figure B.3: Different concentration of CO_2 loading in different concentrations of water and organic solvent

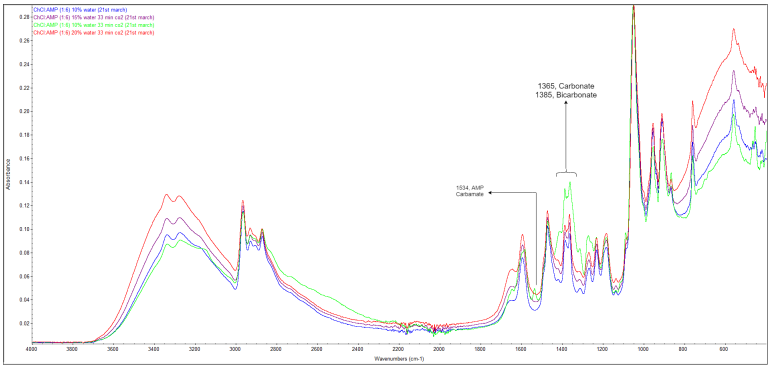

Figure B.4: FTIT plot for ChCl:AMP (1:6) solution with different concentration of H_2O and different concentrations of CO_2

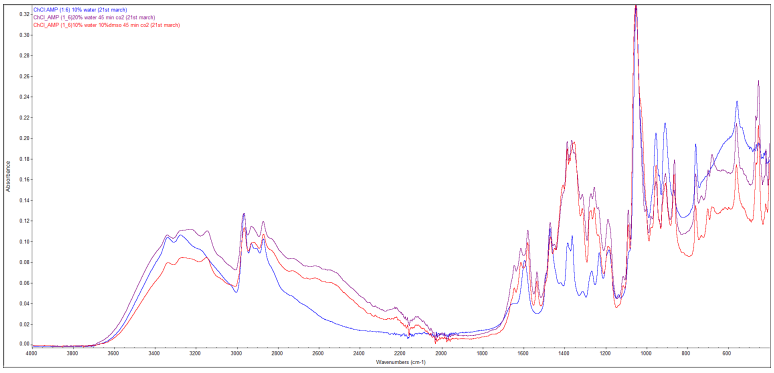

Figure B.5: FTIT plot for ChCl:AMP (1:6) solution and different concentrations of CO_2 in presense of organic solvent

B.3. Mathematical fit for physical parameters

B.3.1. Viscosity

Figure B.6 shows 3D plots for ChCl:MEA(1:6) obtained from table 4.2.

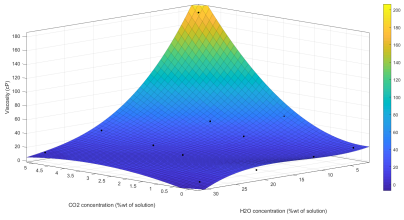

(a) Change in viscosity with different concentration of H_2O and CO_2 at 313.15 K for ChCL:MEA(1:6) solution

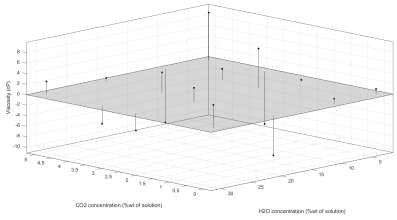

(b) Residual plot for viscosity curve of ChCL:MEA(1:6) solution with different concentrations of H_2O and CO_2 at 323.15 K

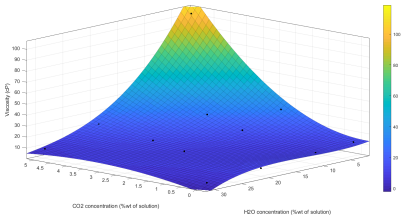

(c) Change in viscosity with different concentration of H_2O and CO_2 at 323.15 K for ChCL:MEA(1:6) solution

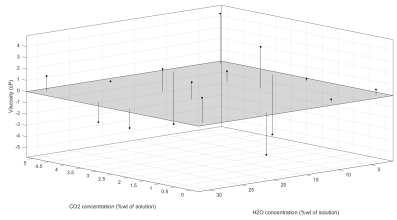

(d) Residual plot for viscosity curve of ChCL:MEA(1:6) solution with different concentrations of H_2O and CO_2 at 323.15 K

Figure B.6: 3D curve for ChCl:MEA(1:6) solution comparing viscosity at different concentration of H_2O and CO_2 at 313.15 K and 323.15 K

Table B.2 shows the predicted values of viscosities for different concentration of water and CO_2 at different temperatures.

B

Table B.2: Predicted values for viscosity of ChCl:MEA(1:6) solution at different temperatures using equation \ref{general equation mea}

Concentration		Viscosity (Temperature) (cP)			
H_2O (%wt of solution)	CO_2 (%wt of solution)	303.15 K	313.15 K	323.15 K	333.15 K
3.00	0.00	29.30	18.69	12.42	8.68
9.95	0.00	22.59	15.25	10.50	7.48
19.99	0.00	31.09	18.24	11.32	7.72
2.92	2.23	83.13	48.10	30.03	20.17
10.02	2.23	31.82	21.52	15.45	11.39
20.69	2.23	20.76	13.98	9.99	7.68
30.31	2.23	19.65	12.65	8.57	6.27
2.92	3.31	150.20	84.82	50.92	33.00
9.94	3.31	64.86	40.26	26.50	18.36
19.90	3.31	25.01	17.29	12.52	9.53
29.83	3.31	21.28	13.67	9.31	6.89
2.92	4.97	303.74	168.90	98.20	61.62
10.11	4.97	147.39	86.50	53.08	34.64
19.90	4.97	44.68	29.43	20.17	14.45
29.79	4.97	12.35	9.21	7.26	5.81

Figure B.7 shows 3D plots for ChCl:AMP(1:6) obtained from table 4.5.

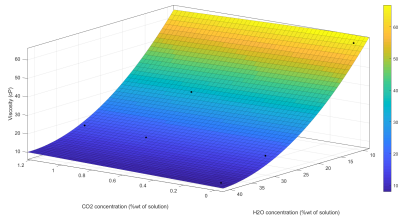

(a) Change in viscosity with different concentration of H_2O and CO_2 at 313.15 K for ChCL:AMP(1:6) solution

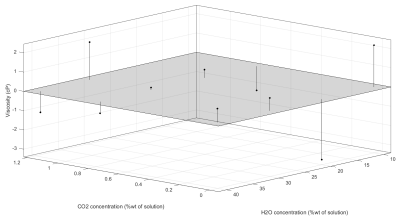

(b) Residual plot for viscosity curve of ChCL:AMP(1:6) solution with different concentrations of H_2O and CO_2 at 313.15 K

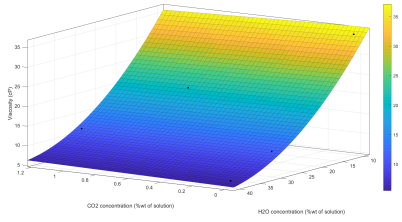

(c) Change in viscosity with different concentration of H_2O and CO_2 at 323.15 K for ChCL:AMP(1:6) solution

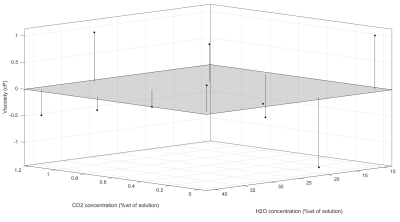

(d) Residual plot for viscosity curve of ChCL:AMP(1:6) solution with different concentrations of H_2O and CO_2 at 323.15 K

Figure B.7: 3D curve for ChCl:AMP(1:6) solution comparing viscosity at different concentration of H_2O and CO_2 at 313.15 K and 323.15 K

Table B.3 shows the predicted values of viscosities for different concentration of water and CO_2 at different temperatures.

Table B.3: Predicted values for viscosity of ChCl:AMP(1:6) solution at different temperatures using equation \ref{general equation AMP}

Concentration		Viscosity (Temperature) (cP)			
H_2O (%wt of solution)	CO_2 (%wt of solution)	303.15 K	313.15 K	323.15 K	333.15 K
10.07	0.00	111.58	61.42	34.43	21.57
20.07	0.00	57.36	33.64	20.57	14.01
30.02	0.00	24.60	16.02	11.10	8.27
40.05	0.00	12.93	8.34	5.91	4.29
10.00	0.77	110.23	59.95	33.63	20.49
19.99	0.77	57.16	33.07	20.20	13.38
30.23	0.77	24.90	15.97	10.95	7.95
39.99	0.77	14.92	9.49	6.37	4.52
30.66	1.16	24.43	15.61	10.67	7.65
40.08	1.16	15.92	10.05	6.57	4.60

B.4. Adding organic solvent

B.4.1. CO_2 loading capacity

Figure B.8 compares the CO_2 absorption of solution with CO_2 purges for 60 min. From the figure, the blue line represents the FTIR spectrum for sample loaded for 60 minutes, and the red line represents the spectrum for sample loaded for 30 minute. From the Figure it is clear that the peak for wavenumber 1307 cm^- increases for sample loaded for more time.

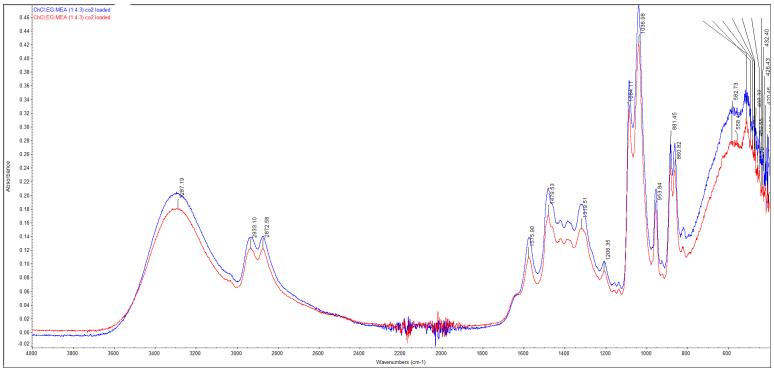

Figure B.8: FTIR plot for CO_2 rich ChCl:EG:MEA(1:3:4) solvent

References

[1] Andrew P. Abbott, John C. Barron, Karl S. Ryder, and David Wilson. Eutectic-based ionic liquids with metal-containing anions and cations. Chemistry - A European Journal, 13(22):6495–6501, 2007.

[2] Climate Change Impacts in the United States: The Third National Climate Assessment. Technical report, U.S. Global Change Research Program, Washington, DC, 2014.

[3] Rebecca Lindsey. Climate Change: Atmospheric Carbon Dioxide | NOAA Climate.gov, 8 2020.

[4] Masoud Hadipoor, Farhad Keivanimehr, Alireza Baghban, Mohammad Reza Ganjali, and Sajjad Habibzadeh. Carbon dioxide as a main source of air pollution: Prospective and current trends to control. In Sorbents Materials for Controlling Environmental Pollution, pages 623–688. Elsevier, 2021.

[5] Wai Lip Theo, Jeng Shiun Lim, Haslenda Hashim, Azizul Azri Mustaffa, and Wai Shin Ho. Review of pre-combustion capture and ionic liquid in carbon capture and storage. Applied Energy, 183:1633–1663, 12 2016.

[6] Xiang Zhang, Zhen Song, Rafiqul Gani, and Teng Zhou. Comparative Economic Analysis of Physical, Chemical, and Hybrid Absorption Processes for Carbon Capture. Cite This: Ind. Eng. Chem. Res, 59, 2020.

[7] Amos Kwabena Dwamena. Investigating Anions and Hydrophobicity of Deep Eutectic Solvents by Experiment and Computational Simulation. Electronic Theses and Dissertations.

[8] Emma L. Smith, Andrew P. Abbott, and Karl S. Ryder. Deep Eutectic Solvents (DESs) and Their Applications, 11 2014.

[9] Shin-ichi Nakao, Katsunori Yogo, Kazuya Goto, Teruhiko Kai, and Hidetaka Yamada. Chemistry of Amine-Based CO2 Capture. Springer, Cham, 5 2019.

[10] Young Eun Kim, Jin Ah Lim, Soon Kwan Jeong, Yeo Il Yoon, Shin Tae Bae, and Sung Chan Nam. Comparison of carbon dioxide absorption in aqueous MEA, DEA, TEA, and AMP solutions. Bulletin of the Korean Chemical Society, 34(3):783–787, 3 2013.

[11] Farouq S. Mjalli, Ghulam Murshid, Suad Al-Zakwani, and Adeeb Hayyan. Monoethanolamine-based deep eutectic solvents, their synthesis and characterization. Fluid Phase Equilibria, 448:30–40, 9 2017.

[12] Zhuo Li, Lili Wang, Changping Li, Yingna Cui, Shenmin Li, Guang Yang, and Yongming Shen. Absorption of Carbon Dioxide Using Ethanolamine-Based Deep Eutectic Solvents. ACS Sustainable Chemistry & Engineering, 7(12):10403–10414, 6 2019.

[13] J.D Seader, Ernest J Henley, and D. Keith Roper. Separation process principles: chemical and biochemical operations. Third edition edition.

[14] Shokat Sarmad, Jyri Pekka Mikkola, and Xiaoyan Ji. Carbon Dioxide Capture with Ionic Liquids and Deep Eutectic Solvents: A New Generation of Sorbents, 1 2017.

[15] Tushar J. Trivedi, Ji Hoon Lee, Hyeon Jeong Lee, You Kyeong Jeong, and Jang Wook Choi. Deep eutectic solvents as attractive media for CO2 capture. Green Chemistry, 18(9):2834–2842, 2016.

[16] M. S. Shaikh, A. M. Shariff, M. A. Bustam, and Ghulam Murshid. Measurement and prediction of physical properties of aqueous sodium L-prolinate and piperazine as a solvent blend for CO2 removal. Chemical Engineering Research and Design, 102:378–388, 10 2015.

[17] Dennis Y.C. Leung, Giorgio Caramanna, and M. Mercedes Maroto-Valer. An overview of current status of carbon dioxide capture and storage technologies, 2014.

[18] Sangeet Nepal, Parth Sarathi Mahapatra, Sagar Adhikari, Sujan Shrestha, Prakash Sharma, Kundan Lal Shrestha, Bidya Banmali Pradhan, and Siva Praveen Puppala. A comparative study of stack emissions from straight-line and zigzag brick kilns in Nepal. Atmosphere, 10(3), 3 2019.

[19] Idowu Adeyemi, Mohammad R.M. Abu-Zahra, and Inas Alnashef. Experimental Study of the Solubility of CO2 in Novel Amine Based Deep Eutectic Solvents. In Energy Procedia, volume 105, pages 1394–1400. Elsevier Ltd, 2017.

[20] J. H. Edwards. Potential sources of CO2 and the options for its large-scale utilisation now and in the future. Catalysis Today, 23(1):59–66, 1 1995.

[21] Jiayou Xu, Zhi Wang, Chenxin Zhang, Song Zhao, Zhihua Qiao, Panyuan Li, Jixiao Wang, and Shichang Wang. Parametric analysis and potential prediction of membrane processes for hydrogen production and pre-combustion CO2 capture. Chemical Engineering Science, 135:202–216, 1 2015.

[22] Lance C. Elwell and Willard S. Grant. Technology options for capturing CO2. Power, 150(8):60–65, 10 2006.

[23] Jawad Mustafa, M Farhan, and M Hussain. CO 2 Separation from Flue Gases Using Different Types of Membranes. Journal of Memberane Science & Technology, 6(2), 6 2016.

[24] Lawien F. Zubeir, Mark H.M. Lacroix, Jan Meuldijk, Maaike C. Kroon, and Anton A. Kiss. Novel pressure and temperature swing processes for CO2 capture using low viscosity ionic liquids. Separation and Purification Technology, 204:314–327, 10 2018.

[25] Adisorn Aroonwilas and Amornvadee Veawab. Characterization and Comparison of the CO2 Absorption Performance into Single and Blended Alkanolamines in a Packed Column. Industrial and Engineering Chemistry Research, 43(9):2228–2237, 4 2004.

[26] Jacob N. Knudsen, Jørgen N. Jensen, Poul Jacob Vilhelmsen, and Ole Biede. Experience with CO2 capture from coal flue gas in pilot-scale: Testing of different amine solvents. Energy Procedia, 1(1):783–790, 2 2009.

[27] Ming Zhao, Andrew I. Minett, and Andrew T. Harris. A review of techno-economic models for the retrofitting of conventional pulverised-coal power plants for post-combustion capture (PCC) of CO2. Energy & Environmental Science, 6(1):25–40, 12 2012.

[28] James Landon and John R. Kitchin. Electrochemical Concentration of Carbon Dioxide from an Oxygen/Carbon Dioxide Containing Gas Stream. Journal of The Electrochemical Society, 157(8):B1149, 6 2010.

[29] Y. Hori. Electrochemical CO<Subscript>2</Subscript> Reduction on Metal Electrodes. Modern Aspects of Electrochemistry, pages 89–189, 3 2008.

[30] Alexander P. Muroyama, Alexandra Pătru, and Lorenz Gubler. ReviewCO 2 Separation and Transport via Electrochemical Methods . Journal of The Electrochemical Society, 167(13):133504, 10 2020.

[31] Peter Wasserscheid and Tom Welton. Ionic Liquids in Synthesis.

[32] Maan Hayyan, Mohd Ali Hashim, Adeeb Hayyan, Mohammed A. Al-Saadi, Inas M. AlNashef, Mohamed E.S. Mirghani, and Olorunnisola Kola Saheed. Are deep eutectic solvents benign or toxic? Chemosphere, 90(7):2193–2195, 2013.

[33] Katherine D. Weaver, Hye Jin Kim, Jiazeng Sun, Douglas R. MacFarlane, and Gloria D. Elliott. Cyto-toxicity and biocompatibility of a family of choline phosphate ionic liquids designed for pharmaceutical applications. Green Chemistry, 12(3):507–51, 3 2010.

[34] Yingying Zhang, Xiaoyan Ji, and Xiaohua Lu. Choline-based deep eutectic solvents for CO2 separation: Review and thermodynamic analysis, 12 2018.

[35] Andrew P. Abbott, Glen Capper, David L. Davies, Raymond K. Rasheed, and Vasuki Tambyrajah. Novel solvent properties of choline chloride/urea mixtures. Chemical Communications, (1):70–71, 2003.

[36] Andrew P. Abbott, Glen Capper, David L. Davies, Helen L. Munro, Raymond K. Rasheed, and Vasuki Tambyrajah. Preparation of novel, moisture-stable, lewis-acidic ionic liquids containing quaternary ammonium salts with functional side chains. Chemical Communications, 1(19):2010–2011, 2001.

[37] Rusul Khaleel Ibrahim, Maan Hayyan, Mohammed Abdulhakim AlSaadi, Shaliza Ibrahim, Adeeb Hayyan, and Mohd Ali Hashim. Physical properties of ethylene glycol-based deep eutectic solvents. Journal of Molecular Liquids, 276:794–800, 2 2019.

[38] Andrew P. Abbott. Application of hole theory to the viscosity of ionic and molecular liquids. ChemPhysChem, 5(8):1242–1246, 8 2004.

[39] Francis Bougie and Maria C. Iliuta. Sterically Hindered Amine-Based Absorbents for the Removal of CO2 from Gas Streams. Journal of Chemical and Engineering Data, 57(3):635–669, 3 2012.

[40] Bihong Lv, Bingsong Guo, Zuoming Zhou, and Guohua Jing. Mechanisms of CO2 Capture into Monoethanolamine Solution with Different CO2 Loading during the Absorption/Desorption Processes. Environmental Science and Technology, 49(17):10728–10735, 9 2015.

[41] Michael Caplow. Kinetics of carbamate formation and breakdown. Journal of the American Chemical Society, 90(24):6795–6803, 2002.

[42] Rhoda B. Leron and Meng Hui Li. Solubility of carbon dioxide in a choline chloride-ethylene glycol based deep eutectic solvent. Thermochimica Acta, 551:14–19, 1 2013.

[43] Yi Hong Hsu, Rhoda B. Leron, and Meng Hui Li. Solubility of carbon dioxide in aqueous mixtures of (relineă+ămonoethanolamine) at Tă=ă(313.2 to 353.2)ăK. The Journal of Chemical Thermodynamics, 72:94–99, 5 2014.

[44] A K Chakraborty, K B Bischoff, G Astarita, and J R Damewood. Molecular Orbital Approach to Substituent Effects in Amine-C02 Interactions. J. Am. Chem. Soc, 110:6947–6954, 1988.

[45] K H KoHoUZ, Guido Sartorl, and David W Savage. Colloid Interface Scl. 197Sa. Physical Chemistry: Enriching Topics from Colloid and Sur-face Science, 22(9):473–482, 1983.

[46] Shin-Ichi Nakao, Katsunori Yogo, Kazuya Goto, Teruhiko Kai, and Hidetaka Yamada. SPRINGER BRIEFS IN ENERGY Advanced CO2 Capture Technologies Absorption, Adsorption, and Membrane Separation Methods.

[47] Martín Avalos, Reyes Babiano, Pedro Cintas, José L. Jiménez, and Juan C. Palacios. Greener Media in Chemical Synthesis and Processing. Angewandte Chemie International Edition, 45(24), 6 2006.

[48] K. Shahbaz, F. S. Mjalli, M. A. Hashim, and I. M. Alnashef. Prediction of deep eutectic solvents densities at different temperatures. Thermochimica Acta, 515(1-2):67–72, 3 2011.

[49] Sushma P. Ijardar. Deep eutectic solvents composed of tetrabutylammonium bromide and PEG: Density, speed of sound and viscosity as a function of temperature. Journal of Chemical Thermodynamics, 140, 1 2020.

[50] Jiyad N. Al-Dawsari, Abdelbasset Bessadok-Jemai, Irfan Wazeer, Salim Mokraoui, Muath A. AlMansour, and Mohamed K. Hadj-Kali. Fitting of experimental viscosity to temperature data for deep eutectic solvents. Journal of Molecular Liquids, 310, 7 2020.

[51] Mohamed Khalid Alomar, Maan Hayyan, Mohammed Abdulhakim Alsaadi, Shatirah Akib, Adeeb Hayyan, and Mohd Ali Hashim. Glycerol-based deep eutectic solvents: Physical properties. Journal of Molecular Liquids, 215:98–103, 3 2016.

[52] Nicolás F. Gajardo-Parra, Michael J. Lubben, Joshua M. Winnert, Ángel Leiva, Joan F. Brennecke, and Roberto I. Canales. Physicochemical properties of choline chloride-based deep eutectic solvents and excess properties of their pseudo-binary mixtures with 1-butanol. Journal of Chemical Thermodynamics, 133:272–284, 6 2019.

[53] Anya F. Bouarab, Jean Philippe Harvey, and Christian Robelin. Viscosity models for ionic liquids and their mixtures, 1 2021.

[54] Divya Dhingra, Bhawna, and Siddharth Pandey. Effect of lithium chloride on the density and dynamic viscosity of choline chloride/urea deep eutectic solvent in the temperature range (303.15358.15) K. Journal of Chemical Thermodynamics, 130:166–172, 1 2019.

[55] Wu Xu and C. Austen Angell. Solvent-Free Electrolytes with Aqueous Solution-Like Conductivities. Science, 302(5644):422–425, 10 2003.

[56] Elena Pérez-Gallent, Chirag Vankani, Carlos Sánchez-Martínez, Anca Anastasopol, and Earl Goetheer. Integrating CO2capture with electrochemical conversion using amine-based capture solvents as electrolytes. Industrial and Engineering Chemistry Research, 60(11):4269–4278, 3 2021.

[57] Gregorio García, Mert Atilhan, and Santiago Aparicio. A theoretical study on mitigation of CO2 through advanced deep eutectic solvents. International Journal of Greenhouse Gas Control, 39:62–73, 8 2015.

[58] Kelly Robinson, Adam McCluskey, and Moetaz I. Attalla. An ATR-FTIR study on the effect of molecular structural variations on the CO2 absorption characteristics of heterocyclic amines, part II. ChemPhysChem, 13(9):2331–2341, 6 2012.

[59] P. Jackson, K. Robinson, G. Puxty, and M. Attalla. In situ Fourier Transform-Infrared (FT-IR) analysis of carbon dioxide absorption and desorption in amine solutions. Energy Procedia, 1(1):985–994, 2 2009.

[60] Helena Svensson, Christian Hulteberg, and Hans T. Karlsson. Precipitation of AMP Carbamate in CO2 Absorption Process. Energy Procedia, 63:750–757, 1 2014.